

# On an active resonant triad of mixed modes in symmetric shear flows: a plane wake as a paradigm

By XUESONG WU

Department of Mathematics, Imperial College, 180 Queens Gate, London SW7 2BZ, UK

(Received 16 September 1995 and in revised form 1 March 1996)

In this paper, we identify a new type of resonant triad which operates in a parallel or nearly parallel shear flow with a symmetric profile. The triad consists of a planar sinuous mode, an oblique sinuous mode and an oblique varicose mode, but is not of the usual subharmonic-resonance form. The development of the triad is studied in the non-equilibrium critical-layer régime. The equations governing the evolution of the modes are derived. We show that the quadratic resonance can significantly enhance the growth of both the oblique sinuous and varicose modes, and may cause them to grow super-exponentially. This can lead to a subsequent stage in which the oblique sinuous mode produces a back reaction on the oblique varicose mode through a phase-locked interaction, causing both oblique modes to evolve even more rapidly. We suggest that the resonant triad is a viable mechanism for the development of three-dimensional structures and varicose components observed in the later stage of plane wake transition.

---

## 1. Introduction

As with boundary layers and mixing layers, plane wakes and jets have been studied extensively during the past few decades because of their practical applications as well as their fundamental importance to the understanding of transition to turbulence. A new aspect associated with such *symmetric* shear flows is that they can support both sinuous and varicose modes; the vertical velocity distribution of the former is symmetric while that of the latter is antisymmetric about the centreline. In the linear régime, two-dimensional sinuous modes have larger growth rates, and hence dominate the initial stage of transition. This earlier stage has been the subject of most previous investigations (e.g. Sato & Kuriki 1961; Sato 1970; Sato & Saito 1975, 1978; Mattingly & Criminale 1972; Ko, Kubota & Lees 1970; Miksad *et al.* 1982).

Recent experimental studies reveal that further downstream, three-dimensional disturbances develop rapidly and become dominant (Cimbala, Nagib & Roshko 1988; Corke, Krull & Ghassemi 1992; Williamson & Prasad 1993*a,b*; see also Sato & Kuriki 1961). Moreover, varicose components are found to attain an appreciable magnitude (Corke *et al.* 1992). The objective of this paper is to propose a viable mechanism for the preferential amplification of (i) varicose modes, and (ii) three-dimensional sinuous modes, observed in the later stage.

The rôle of varicose modes does not seem to have received sufficient theoretical attention. They are often disregarded on the grounds that they have a smaller linear growth rate. However, Wagnanski, Champagne & Marasli (1986) found that although

the prevailing instability is sinuous in nature, a small varicose component can alter the gross features of the flow pattern. In order for the calculated streamline to mimic the observed flow structure in experiments, varicose components have to be included. Further investigations of Marasli, Champagne & Wygnanski (1989) show that a varicose mode with a magnitude half that of the sinuous mode can be sustained in the flow far downstream.

The interaction between a nearly neutral (two-dimensional) sinuous mode and a nearly neutral (two-dimensional) varicose mode in a special symmetric shear flow, the Bickley jet, was considered by Leib & Goldstein (1989). For such a profile, the latter mode is the subharmonic of the former, and hence they satisfy Kelly's (1968) resonance condition. Leib & Goldstein investigated such a resonance in the non-equilibrium, (strongly) nonlinear critical-layer régime, and found that the development of the varicose mode was either suppressed or hardly affected by the sinuous mode. This implies that the Kelly type of resonance cannot induce the observed development of varicose modes. For a general symmetric profile, it is not known whether a planar (nearly) neutral varicose mode is the subharmonic of the planar sinuous mode, and so even the existence of the Kelly type of resonance is an open question.

As indicated above, another concern of this paper is with the rapid development of three-dimensional disturbances. Usually the subharmonic resonant-triad interaction, which was originally proposed by Raetz (1959) and Craik (1971), provides a possible explanation. Indeed, recent studies of such a mechanism have improved our understanding of three-dimensional transition processes in boundary layers as well as in other shear flows; see for example Goldstein & Lee (1992), Wu (1992, 1993, 1995), Mankbadi, Wu & Lee (1993), Wundrow, Hultgren & Goldstein (1994), Lee (1994) and Mallier & Maslowe (1994). However, in a symmetric shear flow such as a plane wake, this mechanism ceases to operate for sinuous modes because the interaction coefficients are identically zero as a result of the symmetry of the flow (see e.g. Wu 1995). Subharmonic resonance is active among appropriate varicose modes, and was studied by Mallier (1995). He further proposes that through mutual interactions, the varicose modes may affect the development of sinuous modes. However, this requires the planar varicose mode to have a magnitude much larger than that of the sinuous modes. Since varicose modes have a much smaller linear growth rate, the scenario suggested by Mallier is unlikely to occur unless the planar varicose mode is preferentially excited by some means. For natural transition, a more viable mechanism for promoting the rapid growth of three-dimensional disturbances has been proposed by Wu & Stewart (1996a). This is the so-called phase-locked interaction among sinuous modes which share the same phase velocity. It is found that this mechanism can explain major experimental observations quite well, although a detailed quantitative comparison is yet to be achieved.

In the present paper, we shall show that while the subharmonic resonance (involving solely sinuous modes) is inactive, there exists an *active* resonant triad of non-subharmonic type which consists of a planar sinuous mode, an oblique sinuous mode and an oblique varicose mode. We show that the resonance significantly enhances the growth of the oblique varicose mode, and may cause both the oblique sinuous and varicose modes to grow super-exponentially even though their magnitudes are infinitesimal. This offers a possible mechanism by which three-dimensional disturbances, particularly disturbances of varicose nature, attain a significant magnitude in the later stage of transition. Compared with the phase-locked interaction of Wu & Stewart (1996a), such a resonant interaction requires a more restrictive condition in the sense that it can only occur among the modes with particular wavenumbers

or frequencies. However, the necessary threshold magnitude of the planar sinuous mode for this resonance to take place is much smaller than that for the phase-locked interaction. Hence the two mechanisms are complementary to each other.

In addition to the quadratic resonance, a phase-locked interaction can take place between the two oblique modes. Namely, the oblique sinuous and varicose modes can interact to generate an exceptionally large difference mode which in turn interacts with the oblique sinuous mode to affect the development of the oblique varicose mode (cf. Wu & Stewart 1996a). This effect will be included in our analysis.

The rest of the paper is organized as follows. In the next section, we show that for the Bickley jet, appropriate sinuous and varicose modes can form a resonant triad. We further show that such a resonant-triad interaction of mixed modes is likely to exist in *any* symmetric shear flow. For this reason, we choose to formulate the problem for a shear flow with an arbitrary symmetric profile. In particular, we consider the evolution of the triad in the so-called non-equilibrium critical layer régime. The appropriate asymptotic scalings are specified. This is followed by a systematic expansion of the solution in the main part of the flow in §3. The flow within the viscous, non-equilibrium critical layers is analysed in §4, where the solutions are obtained analytically. Matching them onto those in the outer region, we obtain the (coupled) amplitude equations (§5). In §6, the general analysis is specialized to a plane wake, and the coefficients involved in the amplitude equations are evaluated explicitly. The amplitude equations are studied in §7, both analytically and numerically. In §8, the implications of the results are discussed and related to experiments on transition of a plane wake. The Appendix contains the analysis of the phase-locked interaction between the two oblique modes.

## 2. Formulation and scalings

The flow is to be described in terms of Cartesian coordinates  $(x, y, z)$ , where  $x$ ,  $y$  and  $z$  are streamwise, transverse and spanwise coordinates respectively. As usual, they are non-dimensionalized by  $\delta^*$ , the thickness of the shear layer at a typical streamwise location, say  $x = 0$ . The time  $t$ , the velocity  $(U, V, W)$  and the pressure  $p$  are non-dimensionalized by  $\delta^*/U_0$ ,  $U_0$  and  $\rho_0 U_0^2$  respectively, where  $U_0$  is a reference velocity and  $\rho_0$  the density of the fluid. The Reynolds number  $R$  is defined as

$$R = \frac{U_0 \delta^*}{\nu},$$

where  $\nu$  is the kinematic viscosity. Throughout this paper, we shall assume that  $R \gg 1$  so that a self-consistent approach can be pursued. The analysis is to be applicable to any inviscidly unstable, almost parallel two-dimensional flow with a velocity profile

$$(\bar{U}(x_3, y), R^{-1} \bar{V}(x_3, y), 0),$$

which will be assumed to be symmetric about  $y = 0$ . The dependence of the mean-flow velocities on the slow variable

$$x_3 = x/R,$$

is associated with the non-parallel flow effect, and is parametric in the present study. This basic flow is perturbed by disturbance  $(u, v, w)$  and the perturbed flow is denoted by

$$(U, V, W) = (\bar{U} + u, R^{-1} \bar{V} + v, w).$$

### 2.1. Existence of an active resonant triad of mixed modes

We are concerned with possible active resonant-triad interaction in symmetric flows. Instead of the subharmonic resonance of varicose modes (Mallier 1995), we look for a different resonant triad in which the planar sinuous mode plays the most active rôle in the sense that it can significantly enhance the growth of the oblique sinuous and varicose modes, in line with experimental observations. In order to be specific, we first consider a special symmetric shear flow with the profile

$$\bar{U} = U_0 - \operatorname{sech}^2 y, \quad (2.1)$$

where  $U_0$  is the free-stream velocity. It is well known that for such a profile, there exist a planar neutral sinuous mode (Drazin & Howard 1966)

$$\alpha_{s0} = 2, \quad c = U_0 - \frac{2}{3}, \quad \bar{\phi}_0 = \operatorname{sech}^2 y, \quad (2.2)$$

and a planar neutral varicose mode

$$\alpha_{v0} = 1, \quad c = U_0 - \frac{2}{3}, \quad \bar{\phi}_v = \sinh y \operatorname{sech}^2 y, \quad (2.3)$$

where  $\alpha_{s0}$  and  $\alpha_{v0}$  are the streamwise wavenumbers of the sinuous and varicose modes respectively, and  $c$  is the phase speed, while  $\bar{\phi}_s$  and  $\bar{\phi}_v$  are the corresponding eigenfunctions of the vertical velocities.

Suppose that  $(\alpha_s, \beta, c_s)$  is an oblique sinuous mode, and  $(\alpha_v, -\beta, c_v)$  an oblique varicose mode. It follows from Squire's transformation that if

$$\alpha_s^2 + \beta^2 = 4, \quad \text{and} \quad \alpha_v^2 + \beta^2 = 1, \quad (2.4)$$

then these two oblique modes are both neutral and have the same phase velocity as the planar sinuous mode  $(\alpha_{s0}, 0, c)$ . It is easy to check that  $(\frac{7}{4}, \frac{1}{4}\sqrt{15}, c)$  and  $(\frac{1}{4}, -\frac{1}{4}\sqrt{15}, c)$  satisfy (2.4), and hence are neutral oblique sinuous and varicose modes respectively. Moreover, the following three modes,

$$(2, 0, c), \quad (\frac{7}{4}, \frac{1}{4}\sqrt{15}, c), \quad (\frac{1}{4}, -\frac{1}{4}\sqrt{15}, c), \quad (2.5)$$

form a resonant triad, since the quadratic interaction between the planar and sinuous modes produces the oblique varicose mode, while the oblique varicose mode interacts with the planar mode to produce the oblique sinuous mode. Note that this is not the usual subharmonic resonance.

Although such a resonant triad of mixed modes is identified for a special profile, it is likely to exist in any symmetric shear flow, as we shall argue below. For a symmetric shear flow, there usually exist a two-dimensional neutral sinuous mode, say  $(\alpha_{s0}, 0, c)$ , and a two-dimensional neutral varicose mode, say  $(\alpha_{v0}, 0, c)$ , where both modes have the same phase speed  $c$  since it equals the basic-flow velocity at the inflexion points. An oblique sinuous mode  $(\alpha_s, \beta, c)$ , and an oblique varicose mode  $(\alpha_v, -\beta, c)$  are also neutral if

$$\alpha_s^2 + \beta^2 = \alpha_{s0}^2, \quad \text{and} \quad \alpha_v^2 + \beta^2 = \alpha_{v0}^2. \quad (2.6)$$

If we further require that

$$\alpha_s + \alpha_v = \alpha_{s0}, \quad (2.7)$$

then the three modes

$$(\alpha_{s0}, 0, c), \quad (\alpha_s, \beta, c), \quad (\alpha_v, -\beta, c), \quad (2.8)$$

or alternatively,

$$(\alpha_{s0}, 0, c), \quad (\alpha_s, -\beta, c), \quad (\alpha_v, \beta, c),$$

form a resonant triad, where

$$\alpha_s = \left(1 - \frac{1}{2} \left(\frac{\alpha_{v0}}{\alpha_{s0}}\right)^2\right) \alpha_{s0}, \quad \alpha_v = \frac{\alpha_{v0}^2}{2\alpha_{s0}}, \quad \beta = \left(1 - \left(\frac{\alpha_{v0}}{2\alpha_{s0}}\right)^2\right)^{1/2} \alpha_{v0}, \quad (2.9)$$

as can be found from (2.6) and (2.7). The first of the above equations indicates that the only condition for the existence of such a triad is

$$\alpha_{s0} > \frac{1}{\sqrt{2}} \alpha_{v0}, \quad (2.10)$$

which can be satisfied in general, since calculations of eigenvalues for different profiles suggest that it is usually the case that  $\alpha_{s0} > \alpha_{v0}$  (Sato & Kuriki 1961; Mattingly & Criminale 1972; Chen, Cantwell & Mansour 1990). We note that in addition to the oblique modes in (2.8), their ‘mirror’ modes can also be included so that the disturbance consists of five waves,

$$(\alpha_{s0}, 0, c), \quad (\alpha_s, \pm\beta, c), \quad (\alpha_v, \pm\beta, c). \quad (2.11)$$

In the régime to be studied in the present paper, such an extended form of disturbance evolves in the same fashion as (2.8), and hence it suffices to consider the resonance among the three waves in (2.8).

The existence of a resonant-triad interaction among mixed modes in a symmetric shear flow is a fundamental observation of this paper. The evolution of the triad can be considered in different asymptotic régimes. In the present paper, we shall study this in the so-called non-equilibrium critical-layer régime as we believe it to be the most relevant to experiments. Moreover, the amplitude equations relevant to other régimes can be obtained by taking an appropriate limit of our results (see §7.1). For a survey of recent studies of non-equilibrium critical layers, the reader is referred to the reviews by Goldstein & Lee (1993), Goldstein (1994) and Cowley & Wu (1994). Since the resonant triad identified above is likely to be generic, we shall first perform the analysis for a symmetric shear flow with an arbitrary profile, and then specialize it to the profile (2.1).

## 2.2. Formulation

When a resonant triad of sufficiently small magnitude is excited upstream, each wave initially evolves exponentially according to linear, quasi-parallel instability theory, and then becomes neutral at some location downstream due to the viscous spreading of the basic flow. For a disturbance in the form of a resonant triad, the three waves become linearly neutral at the same streamwise location. Near such a location, the disturbance has attained the maximum magnitude through linear growth. Moreover, as the disturbance becomes nearly neutral, critical layers emerge and nonlinear interactions between the modes can first take place there, as recent studies have shown (e.g. Goldstein & Lee 1992; Wu 1992; Goldstein 1994; Cowley & Wu 1994). Therefore, it is appropriate to assume that nonlinear effects become important slightly upstream of the linearly neutral station. The local growth rate is small, of order  $\mu$  say, and the local frequencies of the three modes deviate from their local neutral values by  $O(\mu)$ . More precisely

$$\omega_{s0} = \alpha_{s0}c + \mu\alpha_{s0}S_0, \quad \omega_s = \alpha_s c + \mu\alpha_s S, \quad \omega_v = \alpha_v c + \mu\alpha_v S_v, \quad (2.12)$$

where  $\omega_{s0}$ ,  $\omega_s$  and  $\omega_v$  are the frequencies of the planar sinuous mode, the oblique sinuous mode and the oblique varicose mode respectively, while  $\alpha_{s0}$ ,  $\alpha_s$  and  $\alpha_v$  are

their wavenumbers. The parameters  $S_0$ ,  $S$ ,  $S_v < 0$  represent the scaled deviations of the phase speeds from the neutral value. In order to accommodate the general case where  $S_0$ ,  $S$  and  $S_v$  are not equal, and also to include the effect of simultaneous temporal–spatial modulation, we introduce a slow time variable

$$T = \mu t . \quad (2.13)$$

For later convenience, we also introduce

$$\zeta = x - ct , \quad (2.14)$$

which is the coordinate travelling with the common phase velocity (to leading order).

To leading order, the disturbance in the main part of the flow field has the form

$$v = \epsilon A_0(x_1, T) \bar{\phi}_0 e^{i\alpha_0 \zeta} + \delta_s A_s(x_1, T) \bar{\phi}_s e^{i(\alpha_s \zeta - \beta z)} + \delta_v A_v(x_1, T) \bar{\phi}_v e^{i(\alpha_v \zeta + \beta z)} + \dots , \quad (2.15)$$

where  $\epsilon$ ,  $\delta_s$ ,  $\delta_v \ll 1$  represent the magnitudes of the three modes respectively, while  $A_0$ ,  $A_s$  and  $A_v$  are the associated amplitude functions, which are allowed to depend on the slow streamwise variable  $x_1 = \mu x$  as well as on the slow time variable  $T$ . A scaling argument similar to that of Wu (1992) shows that when

$$\epsilon = O(\mu^4) , \quad (2.16)$$

a resonance takes place among the three waves. It follows from (2.16) that the slow time variable  $T$  and the slow streamwise variable  $x_1$  should be defined as

$$T = \epsilon^{1/4} t , \quad x_1 = \epsilon^{1/4} c^{-1} x , \quad (2.17)$$

where the factor  $c^{-1}$  is introduced for later convenience. If  $\alpha_{s0} > \alpha_{v0}$ , our scaling argument further shows that when

$$\delta_s \sim \delta_v = O(\epsilon^{7/8}) , \quad (2.18)$$

the oblique sinuous mode will produce a feedback effect on the varicose mode through a phase-locked interaction (cf. Wu & Stewart 1996a). This interaction, however, is negligible when

$$\delta_s \sim \delta_v \ll O(\epsilon^{7/8}) . \quad (2.19)$$

The régime with the above restriction will be referred to as the parametric resonance stage. We shall show that in this stage, both the oblique sinuous and varicose modes experience super-exponential growth, while the plane mode still evolves exponentially.

Given that the two oblique modes have smaller linear growth rates, for natural transition (2.19) is likely to hold at the beginning of the parametric resonance. However, the oblique modes may attain the magnitude specified by (2.18), either because of initial forcing or as a result of the super-exponential growth in the parametric resonance stage. Thus, we shall adopt the scaling (2.18) so as to include the effect of the phase-locked interaction. We note that even if the mirror mode of each oblique mode is included, there will be no interaction between the modes in each pair, since for such an interaction to occur, the oblique modes must have a magnitude of  $O(\epsilon^{3/4})$ , much larger than that prescribed by (2.18) (cf. Goldstein & Choi 1989; Wu, Lee & Cowley 1993; Wu & Stewart 1996a).

In order to investigate the viscous effect, we consider the distinguished case where viscous diffusion terms appear at leading-order in the critical-layer equations. This occurs when (cf. Wu *et al.* 1993)

$$R^{-1} = \lambda \epsilon^{3/4} , \quad (2.20)$$

where the parameter  $\lambda$  characterizes the relative importance of viscosity to nonlinear effects (cf. Haberman 1972). Throughout §§3–6,  $\lambda$  will be assumed to be of order one so that the critical layers are both viscous and non-equilibrium in nature. The highly viscous case corresponding to  $\lambda$  being asymptotically large will be discussed in §7.1

The basic flow  $\bar{U}$  evolves on the very slow streamwise variable  $x_3$ , and it is sufficient to approximate its profile at  $x_3$  as a Taylor expansion about  $x_3 = 0$ :

$$\bar{U}(y, x_3) = \bar{U}(y) + \frac{\partial \bar{U}}{\partial x_3} x_3 + \dots = \bar{U}(y) + \lambda \epsilon^{1/2} x_1 \bar{U}_1(y) + \dots, \tag{2.21}$$

where the term  $\lambda \epsilon^{1/2} x_1 \bar{U}_1(y)$  represents the non-parallel flow correction.

### 3. Outer solution and solvability conditions

Outside the critical layers, the unsteady flow is basically linear and inviscid. The velocity  $(u, v, w)$  and the pressure  $p$  of the disturbance are expanded as

$$u = \epsilon(-i\alpha_{s0})^{-1} \phi'_0 + \delta u_s + \delta u_v + \delta^2 \mu^{-3} u_f + \dots, \tag{3.1}$$

$$v = \epsilon \phi_0 + \delta \phi_s + \delta \phi_v + \epsilon^{5/4} \phi_0^{(1)} + \delta \epsilon^{1/4} \phi_s^{(1)} + \delta \epsilon^{1/4} \phi_v^{(1)} + \delta^2 \mu^{-3} v_f + \dots, \tag{3.2}$$

$$w = \delta w_s + \delta w_v + \delta^2 \mu^{-3} w_f + \dots, \tag{3.3}$$

$$p = \epsilon p_0 + \delta p_s + \delta p_v + \delta^2 \mu^{-3} p_f + \dots, \tag{3.4}$$

where  $\delta = \delta_s = \delta_v$ . In the expansion, we have only retained those terms that will be relevant for the derivation of the amplitude equations.

The disturbance starts from the linear stage upstream and evolves downstream to the régime where the resonant interactions take place. Guided by the earlier linear solution, in the nonlinear stage we seek solutions of the form

$$\phi_0 = A_0(x_1, T) \bar{\phi}_0(y) e^{i\alpha_{s0}\zeta} + \text{c.c.}, \tag{3.5}$$

$$\phi_s = A_s(x_1, T) \bar{\phi}_s(y) e^{i(\alpha_s\zeta - \beta z)} + \text{c.c.}, \tag{3.6}$$

$$\phi_v = A_v(x_1, T) \bar{\phi}_v(y) e^{i(\alpha_v\zeta + \beta z)} + \text{c.c.}, \tag{3.7}$$

where  $\bar{\phi}_0$ ,  $\bar{\phi}_s$  and  $\bar{\phi}_v$  are the eigenfunctions of the three modes. The functions  $\bar{\phi}_0$  and  $\bar{\phi}_v$  satisfy Rayleigh's equations

$$L(\alpha_{s0}, c) \bar{\phi}_0 = 0, \quad L(\bar{\alpha}_v, c) \bar{\phi}_v = 0, \tag{3.8}$$

where  $\bar{\alpha}_v = (\alpha_v^2 + \beta^2)^{1/2}$ , and

$$L(\alpha, c) = \left( \frac{\partial^2}{\partial y^2} - \alpha^2 \right) - \frac{\bar{U}'''}{\bar{U} - c}, \tag{3.9}$$

which is parameterized by  $\alpha$  and  $c$ . The boundary conditions are

$$\bar{\phi}_0 \rightarrow 0, \quad \bar{\phi}_v \rightarrow 0 \quad \text{as } y \rightarrow \pm\infty.$$

Let  $\eta = y - y_c^j$ , where  $y_c^j$  is the  $j$ th critical level at which  $\bar{U} = c$ . Since the profile under consideration is symmetric,  $j = 1, 2$ . The two critical layers are located at the inflexion points; so  $\bar{U}'' = 0$ . As  $\eta \rightarrow \pm 0$ ,

$$\bar{\phi}_0 \rightarrow b_j + a_j \eta + \frac{1}{2} \left( \alpha_{s0}^2 + \frac{\bar{U}'''}{\bar{U}'_c} \right) \eta^2 + \dots, \tag{3.10}$$

$$\bar{\phi}_v \rightarrow \hat{b}_j + \hat{a}_j \eta + \frac{1}{2} \left( \bar{\alpha}_v^2 + \frac{\bar{U}'''}{\bar{U}'_c} \right) \eta^2 + \dots. \tag{3.11}$$

Because the eigenfunctions of the sinuous and varicose modes,  $\bar{\phi}_0$  and  $\bar{\phi}_v$ , are symmetric and antisymmetric about  $y = 0$  respectively, we have

$$b_1 = b_2 = b, \quad a_1 = -a_2 = a, \tag{3.12}$$

$$\hat{b}_1 = -\hat{b}_2 = \hat{b}, \quad \hat{a}_1 = \hat{a}_2 = \hat{a}. \tag{3.13}$$

The function  $\bar{\phi}_s$  satisfies the same equation as  $\bar{\phi}_0$  except that  $\alpha_{s0}$  in (3.8) is replaced by

$$\bar{\alpha}_s = (\alpha_s^2 + \beta^2)^{1/2}.$$

Since it is assumed that  $\alpha_{s0} = \bar{\alpha}_s$ , it follows that

$$\bar{\phi}_s \equiv \bar{\phi}_0.$$

The solutions for  $\phi_0^{(1)}$ ,  $\phi_s^{(1)}$  and  $\phi_v^{(1)}$  (see (3.2)) can be written as

$$\phi_0^{(1)} = \bar{\phi}_0^{(1)}(y, x_1, T) e^{i\alpha_{s0}\zeta} + \text{c.c.}, \tag{3.14}$$

$$\phi_s^{(1)} = \bar{\phi}_s^{(1)}(y, x_1, T) e^{i(\alpha_s\zeta - \beta z)} + \text{c.c.}, \tag{3.15}$$

$$\phi_v^{(1)} = \bar{\phi}_v^{(1)}(y, x_1, T) e^{i(\alpha_s\zeta + \beta z)} + \text{c.c.} \tag{3.16}$$

The function  $\bar{\phi}_0^{(1)}$  satisfies the inhomogeneous Rayleigh equation,

$$L(\alpha_{s0}, c)\bar{\phi}_0^{(1)} = -2i\alpha_{s0}c^{-1} \frac{\partial A_0}{\partial x_1} \bar{\phi}_0 + i\alpha_{s0}^{-1} \left[ \frac{\partial A_0}{\partial T} + \frac{\partial A_0}{\partial x_1} \right] \frac{\bar{U}''}{(\bar{U} - c)^2} \bar{\phi}_0. \tag{3.17}$$

As  $\eta \rightarrow \pm 0$ ,

$$\bar{\phi}_0^{(1)} \rightarrow d_j^\pm + c_j^\pm \eta + b_j s_j \eta \log |\eta| + \dots, \tag{3.18}$$

where  $c_j^\pm$  and  $d_j^\pm$  are as yet unknown functions of  $x_1$  and  $T$ , and

$$s_j = (i\alpha_{s0})^{-1} \left[ -\frac{\partial A_0}{\partial x_1} - \frac{\partial A_0}{\partial T} \right] \frac{\bar{U}_c'''}{\bar{U}_c'^2}. \tag{3.19}$$

Multiplying both sides of (3.17) by  $\bar{\phi}_0$ , and integrating from  $-\infty$  to  $+\infty$ , we obtain the solvability condition for (3.17)

$$\sum_j b_j (c_j^+ - c_j^-) = 2i\alpha_{s0}c^{-1} \tilde{J}_1 \frac{\partial A_0}{\partial x_1} - i\alpha_{s0}^{-1} \left[ \frac{\partial A_0}{\partial x_1} + \frac{\partial A_0}{\partial T} \right] \tilde{J}_2, \tag{3.20}$$

where the sum is over the two critical layers, and  $\tilde{J}_1$  and  $\tilde{J}_2$  are constants defined by

$$\tilde{J}_1 = \int_{-\infty}^{+\infty} \bar{\phi}_0^2 dy, \quad \tilde{J}_2 = \int_{-\infty}^{+\infty} \frac{\bar{U}'' \bar{\phi}_0^2}{(\bar{U} - c)^2} dy, \tag{3.21}$$

with  $\tilde{J}_2$  being interpreted as a Cauchy principal value.

The functions  $\bar{\phi}_s^{(1)}$  and  $\bar{\phi}_v^{(1)}$  satisfy equations similar to (3.17), and hence as  $\eta \rightarrow \pm 0$ ,

$$\bar{\phi}_s^{(1)} \rightarrow \tilde{d}_j^\pm + \tilde{c}_j^\pm \eta + b_j \tilde{s}_j \eta \log |\eta| + \dots, \tag{3.22}$$

$$\bar{\phi}_v^{(1)} \rightarrow \hat{d}_j^\pm + \hat{c}_j^\pm \eta + \hat{b}_j \hat{s}_j \eta \log |\eta| + \dots, \tag{3.23}$$

where  $\tilde{s}_j$  and  $\hat{s}_j$  have the same expressions as  $s_j$  except that  $\alpha_{s0}$  is replaced by  $\alpha_s$ ,  $\alpha_v$ , and  $A_0$  is replaced by  $A_s$  and  $A_v$  respectively. The solvability conditions for  $\bar{\phi}_s^{(1)}$  and



$\bar{\phi}_v^{(1)}$  lead to

$$\sum_j b_j(\hat{c}_j^+ - \hat{c}_j^-) = 2i\alpha_s c^{-1} \hat{J}_1 \frac{\partial A_s}{\partial x_1} - i\alpha_s^{-1} \left[ \frac{\partial A_s}{\partial x_1} + \frac{\partial A_s}{\partial T} \right] \hat{J}_2, \tag{3.24}$$

$$\sum_j \hat{b}_j(\hat{c}_j^+ - \hat{c}_j^-) = 2i\alpha_v c^{-1} \hat{J}_1 \frac{\partial A_v}{\partial x_1} - i\alpha_v^{-1} \left[ \frac{\partial A_v}{\partial x_1} + \frac{\partial A_v}{\partial T} \right] \hat{J}_2, \tag{3.25}$$

where

$$\hat{J}_1 = \int_{-\infty}^{+\infty} \bar{\phi}_v^2 \, dy, \quad \hat{J}_2 = \int_{-\infty}^{+\infty} \frac{\bar{U}'' \bar{\phi}_v^2}{(\bar{U} - c)^2} \, dy. \tag{3.26}$$

The jumps  $(c_j^+ - c_j^-)$ ,  $(\hat{c}_j^+ - \hat{c}_j^-)$  and  $(\hat{c}_j^+ - \hat{c}_j^-)$  in (3.20), (3.24) and (3.25) are to be determined in the next section by a detailed analysis of the dynamics within the critical layers.

We now seek the solutions for the pressure, and the streamwise and spanwise velocities of the disturbance. The leading-order solutions for the pressure of the three modes take the form

$$p_0 = A_0(x_1, T) \bar{p}_0 e^{i\alpha_0 \zeta} + \text{c.c.}, \tag{3.27}$$

$$p_s = A_s(x_1, T) \bar{p}_s e^{i(\alpha_s \zeta - \beta z)} + \text{c.c.}, \tag{3.28}$$

$$p_v = A_v(x_1, T) \bar{p}_v e^{i(\alpha_v \zeta + \beta z)} + \text{c.c.} \tag{3.29}$$

It is found that as  $\eta \rightarrow \pm 0$ ,

$$\bar{p}_0 \rightarrow i\alpha_{s0}^{-1} \bar{U}'_c b_j + \dots, \tag{3.30}$$

$$\bar{p}_s \rightarrow i\bar{\alpha}_s^{-1} \bar{U}'_c \cos \theta b_j + \dots, \tag{3.31}$$

$$\bar{p}_v \rightarrow i\bar{\alpha}_v^{-1} \bar{U}'_c \cos \theta_v \hat{b}_j + \dots, \tag{3.32}$$

where we have defined

$$\theta = \tan^{-1} \beta / \alpha_s, \quad \theta_v = \tan^{-1} \beta / \alpha_v.$$

It follows from the continuity equation that the streamwise velocity of the planar mode is  $(-i\alpha_{s0})^{-1} \bar{\phi}'_0$ . The solutions for the streamwise and spanwise velocities of the sinuous oblique mode,  $u_s$  and  $w_s$ , take the form

$$u_s = A_s(x_1, T) \bar{u}_s e^{i(\alpha_s \zeta - \beta z)} + \text{c.c.}, \quad w_s = iA_s(x_1, T) \bar{w}_s e^{i(\alpha_s \zeta - \beta z)} + \text{c.c.} \tag{3.33}$$

As in Wu (1992), it can be shown that as  $\eta \rightarrow \pm 0$ ,

$$\bar{u}_s \rightarrow -(i\alpha_s)^{-1} \sin^2 \theta b_j \eta^{-1} + \dots, \tag{3.34}$$

$$\bar{w}_s \rightarrow \bar{\alpha}_s^{-1} \sin \theta b_j \eta^{-1} + \dots. \tag{3.35}$$

Similarly, the streamwise and the spanwise velocities of the oblique varicose mode,  $u_v$  and  $w_v$ , can be written as

$$u_v = A_v(x_1, T) \bar{u}_v e^{i(\alpha_v \zeta + \beta z)} + \text{c.c.}, \quad w_v = -iA_v(x_1, T) \bar{w}_v e^{i(\alpha_v \zeta + \beta z)} + \text{c.c.},$$

and as  $\eta \rightarrow \pm 0$ ,

$$\bar{u}_v \rightarrow -(i\alpha_v)^{-1} \sin^2 \theta_v \hat{b}_j \eta^{-1} + \dots, \tag{3.36}$$

$$\bar{w}_v \rightarrow \bar{\alpha}_v^{-1} \sin \theta_v \hat{b}_j \eta^{-1} + \dots. \tag{3.37}$$

The  $O(\delta^2 \mu^{-3})$  terms in (3.1)–(3.4) with the subscript  $f$  are associated with the

difference mode forced by the quadratic interaction between the two oblique modes within the critical layer. They have the form

$$(u_f, v_f, w_f, p_f) = (\bar{u}_f, \bar{v}_f, i\bar{w}_f, \bar{p}_f) e^{i(\alpha_f \zeta - 2\beta z)} + \text{c.c.},$$

where  $\alpha_f = \alpha_s - \alpha_v$ . The function  $\bar{v}_f$  satisfies

$$L(\bar{\alpha}_f, c)\bar{v}_f = 0,$$

where  $\bar{\alpha}_f = (\alpha_f^2 + 4\beta^2)^{1/2}$ . As  $\eta \rightarrow \pm 0$ ,

$$\bar{v}_f \rightarrow D_j + C_j^\pm \eta + \dots, \quad (3.38)$$

where  $C_j^\pm$  and  $D_j$  are functions of  $x_1$  and  $T$ , and the jump  $(C_j^+ - C_j^-)$  in (3.38) is given by (A 5), the right-hand side of which acts as a forcing term to generate  $\bar{v}_f$ .

The solutions for  $\bar{u}_f$ ,  $\bar{w}_f$  and  $\bar{p}_f$  are similar to  $\bar{u}_s$ ,  $\bar{w}_s$  and  $\bar{p}_s$  (see (3.34), (3.35) and (3.31)), except that  $\alpha_s$ ,  $\bar{\alpha}_s$ ,  $b_j$  and  $\theta_s$  are replaced by  $\alpha_f$ ,  $\bar{\alpha}_f$ ,  $D_j$  and  $\theta_f$  respectively, where

$$\theta_f = \tan^{-1} 2\beta/\alpha_f.$$

Because of the symmetry relations (3.12) and (3.13), and the fact that

$$\bar{U}'_c(y_c) = -\bar{U}'_c(-y_c),$$

$A_f$ , defined by (A 6), takes the same value at the two critical levels; so in view of (A 5), we can write

$$C_j^\pm(x_1, T) = \hat{C}_j^\pm A_f(x_1, T), \quad D_j(x_1, T) = \hat{D}_j A_f(x_1, T), \quad (3.39)$$

where  $\hat{C}_j^\pm$  and  $\hat{D}_j$  are constants. The jump (A 5) now simplifies to

$$\hat{C}_j^+ - \hat{C}_j^- = 1. \quad (3.40)$$

The function  $\bar{v}_f$  can be written as

$$\bar{v}_f = A_f(x_1, T)\hat{v}_f,$$

where it transpires that  $A_f(x_1, T)$  is essentially the amplitude function of the forced difference mode. The function  $\hat{v}_f$  depends on  $y$  only and satisfies

$$L(\bar{\alpha}_f, c)\hat{v}_f = 0. \quad (3.41)$$

As  $\eta \rightarrow \pm 0$ ,

$$\hat{v}_f \rightarrow \hat{D}_j + \hat{C}_j^\pm \eta + \dots. \quad (3.42)$$

The symmetry of  $\bar{U}(y)$  and the jump (3.40) imply that the forced difference mode,  $\hat{v}_f$ , is symmetric about  $y = 0$ . Hence we have

$$\hat{D}_1 = \hat{D}_2 = \hat{D}.$$

Equation (3.41) subject to (3.42) and (3.40) can be solved to determine  $\hat{D}$ , which will be needed in evaluating one of the coefficients in the amplitude equations.

#### 4. Inner expansion

Within the  $j$ th critical layer, the appropriate local transverse coordinate is

$$Y = (y - y_c^j)/\mu.$$

The expansion takes the following form:

$$u = \delta\mu^{-1}[\hat{U}_s e^{i(\alpha_s\zeta - \beta z)} + \hat{U}_v e^{i(\alpha_v\zeta + \beta z)} + \text{c.c.}] + \delta^2\mu^{-4}[\hat{U}_f e^{i(\alpha_f\zeta - 2\beta z)} + \text{c.c.}] + \delta^2\mu^{-3}U_1 + \delta\mu U_2 + \dots, \quad (4.1)$$

$$v = \epsilon[\hat{A}_0(x_1) e^{i\alpha_0\zeta} + \text{c.c.}] + \delta[\hat{A}_s(x_1) e^{i(\alpha_s\zeta - \beta z)} + \hat{A}_v(x_1) e^{i(\alpha_v\zeta + \beta z)} + \text{c.c.}] + \delta^2\mu^{-3}[D_j e^{i(\alpha_f\zeta - 2\beta z)} + \text{c.c.}] + \delta^2\mu^{-2}V_1 + \epsilon\mu^2 V_2 + \delta\mu^2 V_3 + \dots, \quad (4.2)$$

$$w = \delta\mu^{-1}[i\hat{W}_s e^{i(\alpha_s\zeta - \beta z)} + i\hat{W}_v e^{i(\alpha_v\zeta + \beta z)} + \text{c.c.}] + \delta^2\mu^{-4}[i\hat{W}_f e^{i(\alpha_f\zeta - 2\beta z)} + \text{c.c.}] + \delta^2\mu^{-3}W_1 + \dots, \quad (4.3)$$

$$p = \epsilon[i\alpha_{s0}^{-1}\bar{U}'_c \hat{A}_0 e^{i\alpha_{s0}\zeta} + \text{c.c.}] + \delta[i\bar{\alpha}_s^{-1}\bar{U}'_c \cos\theta \hat{A}_s e^{i(\alpha_s\zeta - \beta z)} + i\bar{\alpha}_v^{-1}\bar{U}'_c \cos\theta_v \hat{A}_v e^{i(\alpha_v\zeta + \beta z)} + \text{c.c.}] + \delta^2\mu^{-3}[i\bar{\alpha}_f^{-1}\bar{U}'_c \cos\theta_f D_j e^{i(\alpha_f\zeta - 2\beta z)} + \text{c.c.}] + \dots, \quad (4.4)$$

where  $\hat{A}_0 = b_j A_0$ ,  $\hat{A}_s = b_j A_s$  and  $\hat{A}_v = \hat{b}_j A_v$ .

It follows from the expansions of the  $x$ - and  $z$ -momentum equations that the leading-order solutions for the streamwise and spanwise velocities of the oblique sinuous mode,  $\hat{U}_s$  and  $\hat{W}_s$ , satisfy the equations,

$$\hat{L}_\alpha \hat{U}_s = -\bar{U}'_c \sin^2\theta \hat{A}_s, \quad \hat{L}_\alpha \hat{W}_s = i\bar{U}'_c \sin\theta \cos\theta \hat{A}_s, \quad (4.5)$$

where we have defined the operator

$$\hat{L}_\alpha = \frac{\partial}{\partial T} + \frac{\partial}{\partial x_1} + i\alpha\bar{U}'_c Y - \lambda \frac{\partial^2}{\partial Y^2} \quad (4.6)$$

with  $\alpha$  acting as a parameter. Solving (4.5) by Fourier transform, we obtain

$$\hat{U}_s = -\bar{U}'_c \sin^2\theta \Pi_s^{(0)}, \quad \hat{W}_s = i\bar{U}'_c \sin\theta \cos\theta \Pi_s^{(0)}, \quad (4.7)$$

where

$$\Pi_s^{(n)} = \int_0^{+\infty} \xi^n \hat{A}_s(x_1 - \xi, T - \xi) e^{-s\xi^3 - i\Omega\xi} d\xi, \quad (4.8)$$

and

$$\Omega = \alpha_s \bar{U}'_c Y, \quad s = \frac{1}{3} \lambda \alpha_s^2 \bar{U}'_c{}^2. \quad (4.9)$$

Similarly, the streamwise and spanwise velocities of the oblique varicose mode,  $\hat{U}_v$  and  $\hat{W}_v$ , are found to be

$$\hat{U}_v = -\bar{U}'_c \sin^2\theta_v \Pi_v^{(0)}, \quad \hat{W}_v = -i\bar{U}'_c \sin\theta_v \cos\theta_v \Pi_v^{(0)}, \quad (4.10)$$

where

$$\Pi_v^{(n)} = \int_0^{+\infty} \xi^n \hat{A}_v(x_1 - \xi, T - \xi) e^{-s_v \xi^3 - i\Omega_v \xi} d\xi, \quad (4.11)$$

and

$$\Omega_v = \alpha_v \bar{U}'_c Y, \quad s_v = \frac{1}{3} \lambda \alpha_v^2 \bar{U}'_c{}^2. \quad (4.12)$$

The  $O(\delta^2\mu^{-4})$  and  $O(\delta^2\mu^{-3})$  terms in (4.1) and (4.3), and  $O(\delta^2\mu^{-2})$  term in (4.2) are associated with the difference mode generated by the interaction between the oblique sinuous and varicose modes. They are only needed for the calculation of the extra contribution to the amplitude equation from the phase-locked interaction. The details concerning those terms are relegated to the Appendix since the focus of this paper is on the resonant-triad interaction.

The vertical velocity at  $O(\epsilon\mu^2)$ ,  $V_2$ , consists of the component of the planar sinuous mode only, namely

$$V_2 = \hat{V}_2 e^{i\alpha_0 \zeta} + \text{c.c.} ,$$

with  $\hat{V}_2$  satisfying

$$\hat{L}_{\alpha_0} \hat{V}_{2,Y Y} = \hat{L}_1(\alpha_{s0}, 0) \hat{A}_0 . \tag{4.13}$$

Here for later convenience, we have defined

$$\hat{L}_1(\alpha, \beta) = (\alpha^2 + \beta^2) \left[ \frac{\partial}{\partial T} + \frac{\partial}{\partial x_1} + i\alpha \bar{U}'_c Y \right] - i\alpha \bar{U}'_c{}'' Y .$$

After solving (4.13) and matching the solution with the outer expansion, we find

$$c_j^+ - c_j^- \equiv \hat{V}_{2,Y}(+\infty) - \hat{V}_{2,Y}(-\infty) = \pi i \operatorname{sgn}(\bar{U}'_c) b_j s_j . \tag{4.14}$$

In order to determine the jumps  $(\hat{c}_j^+ - \hat{c}_j^-)$  and  $(\hat{c}_j^+ - \hat{c}_j^-)$ , we need to solve for the vertical velocity  $V_3$  at  $O(\delta\mu^2)$  (see (4.2)). It can be written as

$$V_3 = \hat{V}_{3s} e^{i(\alpha_s \zeta - \beta z)} + \hat{V}_{3v} e^{i(\alpha_v \zeta + \beta z)} + \text{c.c.} , \tag{4.15}$$

with  $\hat{V}_{3s}$  and  $\hat{V}_{3v}$  satisfying

$$\hat{L}_{\alpha_s} \hat{V}_{3s,Y Y} = \hat{L}_1(\alpha_s, \beta) \hat{A}_s + i\alpha_{s0} \alpha_s^2 \bar{U}'_c{}^3 \sin^2 \theta_v \hat{A}_0 \Pi_v^{*(2)} , \tag{4.16}$$

$$\hat{L}_{\alpha_v} \hat{V}_{3v,Y Y} = \hat{L}_1(\alpha_v, \beta) \hat{A}_v + i\alpha_{s0} \alpha_s^2 \bar{U}'_c{}^3 \sin^2 \theta \hat{A}_0 \Pi_s^{*(2)} + R_p . \tag{4.17}$$

The forcing term  $R_p$  in (4.17) is contributed by the interaction between the oblique sinuous mode and the forced difference mode. It is found that

$$R_p = \frac{1}{2} i\alpha_{s0} \alpha_f^2 \bar{U}'_c{}^3 \sin^2 \theta_f [A_s \Pi_f^{*(2)} + 2i\alpha_{s0} (\alpha_f^2 \bar{U}'_c)^{-1} \sin^2 \theta (\Pi_s^{(0)} \Pi_f^{*(0)})_Y] , \tag{4.18}$$

where  $\Pi_f^{(0)}$  and  $\Pi_f^{(2)}$  are defined by (A2). Equations (4.16) and (4.17) are solved again by Fourier transform to obtain  $\hat{V}_{3s,Y Y}$  and  $\hat{V}_{3v,Y Y}$  respectively. Matching  $\hat{V}_{3s,Y}$  and  $\hat{V}_{3v,Y}$  with their corresponding outer solutions gives

$$\hat{c}_j^+ - \hat{c}_j^- = \hat{V}_{3s,Y}(+\infty) - \hat{V}_{3s,Y}(-\infty) = \pi i \operatorname{sgn}(\bar{U}'_c) b_j \hat{s}_j + h_s N_s , \tag{4.19}$$

$$\hat{c}_j^+ - \hat{c}_j^- = \hat{V}_{3v,Y}(+\infty) - \hat{V}_{3v,Y}(-\infty) = \pi i \operatorname{sgn}(\bar{U}'_c) \hat{b}_j \hat{s}_j + h_v N_v + h_p N_p , \tag{4.20}$$

where

$$h_s = 2\pi i \alpha_{s0} \alpha_s^2 \alpha_v^{-1} \bar{U}'_c |\bar{U}'_c| \sin^2 \theta_v ,$$

$$h_v = 2\pi i \alpha_{s0} \alpha_s^2 \alpha_v^{-1} \bar{U}'_c |\bar{U}'_c| \sin^2 \theta ,$$

$$h_p = \pi i \alpha_{s0} \alpha_f^2 \alpha_v^{-1} \bar{U}'_c |\bar{U}'_c| \sin^2 \theta_f ,$$

$$N_s = \int_0^{+\infty} \xi^2 e^{-s\sigma_v \xi^3} \hat{A}_0(x_1 - \xi, T - \xi) \hat{A}_v^*(x_1 - \sigma_v \xi, T - \sigma_v \xi) d\xi , \tag{4.21}$$

$$N_v = \int_0^{+\infty} \xi^2 e^{-s\sigma_v \xi^3} \hat{A}_0(x_1 - \sigma \xi, T - \sigma \xi) \hat{A}_s^*(x_1 - \sigma_v \xi, T - \sigma_v \xi) d\xi , \tag{4.22}$$

$$N_p = \int_0^{+\infty} K_c(\xi) \hat{A}_s(x_1 - \sigma_f \xi, T - \sigma_f \xi) D_j^*(x_1 - \sigma \xi, T - \sigma \xi) d\xi . \tag{4.23}$$

Here, the constants  $\sigma$ ,  $\sigma_v$ , etc. are defined in (A 8), and the kernel

$$K_c(\xi) = \xi^2 e^{-s_f \sigma \xi^3} + 2\alpha_{s0} \alpha_v^{-1} \sin^2 \theta \int_0^\xi (\xi - \xi) e^{-s \sigma_f^3 \xi^3 - s_f(\sigma_f \xi + \xi)^3 - s_f \sigma_f (\xi - \xi)^3} d\xi, \quad (4.24)$$

with  $s_f$  given by (A3).

### 5. Amplitude equations

Substituting the jump (4.19) into (3.24) and using (4.21), we obtain the following amplitude equation for the oblique sinuous mode:

$$\frac{\partial A_s}{\partial T} + \tilde{c}_g \frac{\partial A_s}{\partial x_1} = \Gamma_s \int_0^{+\infty} \xi^2 e^{-s \sigma_v \xi^3} A_0(x_1 - \xi, T - \xi) A_v^*(x_1 - \sigma_v \xi, T - \sigma_v \xi) d\xi. \quad (5.1)$$

The coefficients  $\tilde{c}_g$  and  $\Gamma_s$  are defined by

$$\tilde{c}_g = \tilde{f}/(-i\alpha_s^{-1} f_s), \quad \Gamma_s = 2h_s b^2 \hat{b}^*/(-i\alpha_s^{-1} f_s),$$

where

$$\tilde{f} = 2i\alpha_s c^{-1} \tilde{J}_1 - i\alpha_s^{-1} f_s, \quad f_s = \tilde{J}_2 + 2\pi i b^2 \frac{\bar{U}_c'''}{\bar{U}_c' \bar{U}_c'}. \quad (5.2)$$

In calculating the coefficients, we have used the symmetry relation (3.12). Throughout this section, the mean-flow quantities,  $\bar{U}_c'$  and  $\bar{U}_c'''$ , take the values at the upper critical layer.

Substituting (4.20) into (3.25), and using (4.22), (4.23), (3.39), (A 6), we obtain the amplitude equation for the oblique varicose mode:

$$\begin{aligned} \frac{\partial A_v}{\partial T} + \hat{c}_g \frac{\partial A_v}{\partial x_1} &= \Gamma_v \int_0^{+\infty} \xi^2 e^{-s \sigma_v \xi^3} A_0(x_1 - \sigma \xi, T - \sigma \xi) A_s^*(x_1 - \sigma_v \xi, T - \sigma_v \xi) d\xi \\ &+ \Gamma_p \int_0^{+\infty} \int_0^{+\infty} K_c(\xi) K_f(\eta) A_s(x_1 - \sigma_f \xi, T - \sigma_f \xi) A_s^*(x_1 - \sigma \xi - \eta, T - \sigma \xi - \eta) \\ &\quad \times A_v(x_1 - \sigma \xi - \sigma \eta, T - \sigma \xi - \sigma \eta) d\xi d\eta, \end{aligned} \quad (5.3)$$

where coefficients  $\hat{c}_g$ ,  $\Gamma_v$  and  $\Gamma_p$  are given by

$$\left. \begin{aligned} \hat{c}_g &= \hat{f}/(-i\alpha_v^{-1} f_v), \quad \Gamma_v = 2h_v |b|^2 \hat{b}/(-i\alpha_v^{-1} f_v), \\ \Gamma_p &= 4\pi^2 \alpha_{s0}^2 \alpha_f^4 \alpha_v^{-2} \sin^2 \theta_f \sin^2 \theta_v \hat{b}^2 |b|^2 \bar{U}_c''^4 \hat{D}/(-i\alpha_v^{-1} f_v), \\ \hat{f} &= 2i\alpha_v c^{-1} \hat{J}_1 - i\alpha_v^{-1} f_v, \quad f_v = \hat{J}_2 + 2\pi i \hat{b}^2 \frac{\bar{U}_c'''}{\bar{U}_c' \bar{U}_c'}; \end{aligned} \right\} \quad (5.4)$$

the kernels  $K_c$  and  $K_f$  are defined by (4.24) and (A 7).

Substitution of (4.14) into (3.20) leads to

$$\frac{\partial A_0}{\partial T} + c_g \frac{\partial A_0}{\partial x_1} = 0, \quad (5.5)$$

where

$$\left. \begin{aligned} c_g &= f/(-i\alpha_{s0}^{-1} f_s), \\ f &= 2i\alpha_{s0} c^{-1} \tilde{J}_1 - i\alpha_{s0}^{-1} f_s. \end{aligned} \right\} \quad (5.6)$$

Equation (5.5) shows that the planar sinuous mode evolves linearly, although it has a finite magnitude as specified by (2.16). The coefficients  $\tilde{c}_g$ ,  $\hat{c}_g$  and  $c_g$  can be

interpreted as the group velocities of the three modes respectively, and take complex values in general.

Note that the analysis presented is valid for any symmetric flow. The coefficients involved in the amplitude equations are expressed in closed forms in terms of the basic-flow profile and the associated solutions of the Rayleigh's equations. The evaluation of these coefficients requires a numerical treatment in general. However, for the profile (2.1), all the coefficients except  $\Gamma_p$  can be calculated analytically, as will be shown in §6.

The appropriate initial condition depends on whether the spectrum of the initial disturbance is discrete or continuous; the latter corresponds to the case where the disturbance consists of three wavepackets. In order to make further progress, we consider the special case where

$$A_s = \tilde{A}_s(x_1) e^{-i\alpha_s S T}, \quad A_v = \tilde{A}_v(x_1) e^{-i\alpha_v S_v T}, \quad A_0 = \tilde{A}_0(x_1) e^{-i\alpha_{s0} S_0 T}, \quad (5.7)$$

and further assume that

$$\alpha_{s0} S_0 - \alpha S = \alpha_v S_v, \quad \text{i.e.} \quad \alpha_s (S_0 - S) = -\alpha_v (S_0 - S_v) \equiv \Delta. \quad (5.8)$$

Nevertheless,  $S$ ,  $S_0$  and  $S_v$  do not necessarily have the same value, i.e. the phase velocities of the three waves can differ by  $O(\mu)$ . Substituting (5.7) into (5.1), (5.3) and (5.5), and using (5.8), we find that  $\tilde{A}_s$ ,  $\tilde{A}_v$  and  $\tilde{A}_0$  are governed by

$$\frac{d\tilde{A}_s}{dx_1} = \kappa_s \tilde{A}_s + \Upsilon_s \int_0^{+\infty} \xi^2 e^{-s\sigma_v \xi^3 + i\sigma_v \Delta \xi} \tilde{A}_0(x_1 - \xi) \tilde{A}_v^*(x_1 - \sigma_v \xi) d\xi, \quad (5.9)$$

$$\begin{aligned} \frac{d\tilde{A}_v}{dx_1} = & \kappa_v \tilde{A}_v + \Upsilon_v \int_0^{+\infty} \xi^2 e^{-s\sigma_v \xi^3 - i\sigma_v \Delta \xi} \tilde{A}_0(x_1 - \sigma \xi) \tilde{A}_s^*(x_1 - \sigma_v \xi) d\xi \\ & + \Upsilon_p \int_0^{+\infty} \int_0^{+\infty} K(\xi, \eta) \tilde{A}_s(x_1 - \sigma_f \xi) \tilde{A}_s^*(x_1 - \sigma \xi - \eta) \tilde{A}_v(x_1 - \sigma \xi - \sigma \eta) d\xi d\eta, \end{aligned} \quad (5.10)$$

$$\frac{d\tilde{A}_0}{dx_1} = \kappa_0 \tilde{A}_0, \quad (5.11)$$

where

$$K(\xi, \eta) = K_c(\xi) K_f(\eta) e^{i\sigma_v \Delta (\xi + \eta)}.$$

The coefficients in the above equations are given by

$$\kappa_s = f_s S / \tilde{f}, \quad \Upsilon_s = 4\pi i \alpha_{s0} \alpha_s^2 \alpha_v^{-1} \bar{U}'_c |\bar{U}'_c| b^2 \hat{b}^* \sin^2 \theta_v / \tilde{f}, \quad (5.12)$$

$$\kappa_v = f_v S_v / \hat{f}, \quad \Upsilon_v = 4\pi i \alpha_{s0} \alpha_s^2 \alpha_v^{-1} \bar{U}'_c |\bar{U}'_c| |b|^2 \hat{b} \sin^2 \theta / \hat{f}, \quad (5.13)$$

$$\Upsilon_p = 4\pi^2 \alpha_{s0}^2 \alpha_f^4 \alpha_v^{-2} \sin^2 \theta_f \sin^2 \theta_v \hat{b}^2 |b|^2 \bar{U}'_c \hat{D} / \hat{f}, \quad (5.14)$$

$$\kappa_0 = f_s S_0 / f. \quad (5.15)$$

In order to match with the linear stage upstream, the amplitudes  $\tilde{A}_s$ ,  $\tilde{A}_v$  and  $\tilde{A}_0$  should have the 'initial' conditions (see e.g. Goldstein & Leib 1989):

$$\tilde{A}_s \rightarrow A_s^{(0)} e^{\kappa_s x_1}, \quad \tilde{A}_v \rightarrow A_v^{(0)} e^{\kappa_v x_1}, \quad \tilde{A}_0 \rightarrow A_0^{(0)} e^{\kappa_0 x_1} \quad \text{as} \quad x_1 \rightarrow -\infty, \quad (5.16)$$

where the complex numbers  $A_s^{(0)}$ ,  $A_v^{(0)}$  and  $A_0^{(0)}$  characterize the scaled initial amplitudes of the three modes respectively. The development of the resonant triad is governed by (5.9), (5.10) and (5.11) together with (5.16).

In order to reduce the number of parameters, we rescale the amplitude equations

by introducing the following new variables:

$$\bar{x} = \kappa_{0r} x_1 - x_0, \quad \bar{\lambda} = \lambda / (\kappa_{0r})^3, \quad \bar{\Delta} = \Delta / \kappa_{0r}, \quad (5.17)$$

$$\bar{A}_s = \tilde{A}_s e^{-i(T_s + \sigma_s^{-1} \kappa_{0i} x_1)} / \lambda_s, \quad (5.18)$$

$$\bar{A}_v = \tilde{A}_v e^{-i(T_v + \sigma_v^{-1} \kappa_{0i} x_1)} / \lambda_v, \quad (5.19)$$

$$\bar{A}_0 = \tilde{A}_0 e^{-i(T_0 + \kappa_{0i} x_1)} |\Upsilon_s| / \kappa_{0r}^4, \quad (5.20)$$

where  $\kappa_{0r}$  and  $\kappa_{0i}$  are the real and imaginary parts of  $\kappa_0$  respectively, and the real constants  $x_0$ ,  $T_0$ ,  $T_s$ ,  $T_v$ ,  $\lambda_s$  and  $\lambda_v$  are chosen to satisfy

$$e^{iT_s} \lambda_s = A_s^{(0)} e^{\bar{\kappa}_s x_0}, \quad e^{iT_v} \lambda_v = A_v^{(0)} e^{\bar{\kappa}_v x_0}, \quad e^{iT_0} \kappa_{0r}^4 / |\Upsilon_s| = A_0^{(0)} e^{x_0},$$

where

$$\bar{\kappa}_s = (\kappa_s - i\sigma_s^{-1} \kappa_{0i}) / \kappa_{0r}, \quad \bar{\kappa}_v = (\kappa_v - i\sigma_v^{-1} \kappa_{0i}) / \kappa_{0r}. \quad (5.21)$$

After rescaling, the amplitude equations and the initial conditions become

$$\frac{d\bar{A}_s}{d\bar{x}} = \bar{\kappa}_s \bar{A}_s + \chi e^{i\phi} \bar{\Upsilon}_s \int_0^{+\infty} \xi^2 e^{-s\sigma_s \xi^3 + i\sigma_s A \xi} \bar{A}_0(\bar{x} - \xi) \bar{A}_v^*(\bar{x} - \sigma_v \xi) d\xi, \quad (5.22)$$

$$\begin{aligned} \frac{d\bar{A}_v}{d\bar{x}} = & \bar{\kappa}_v \bar{A}_v + \chi^{-1} e^{i\phi} \bar{\Upsilon}_v \int_0^{+\infty} \xi^2 e^{-s\sigma_v \xi^3 - i\sigma_v A \xi} \bar{A}_0(\bar{x} - \sigma \xi) \bar{A}_s^*(\bar{x} - \sigma_v \xi) d\xi \\ & + \tilde{\chi} \bar{\Upsilon}_p \int_0^{+\infty} \int_0^{+\infty} K(\xi, \eta) \bar{A}_s(\bar{x} - \sigma_f \xi) \bar{A}_s^*(\bar{x} - \sigma \xi - \eta) \bar{A}_v(\bar{x} - \sigma \xi - \sigma \eta) d\xi d\eta, \end{aligned} \quad (5.23)$$

$$\frac{d\bar{A}_0}{d\bar{x}} = \bar{A}_0, \quad (5.24)$$

$$\bar{A}_s \rightarrow e^{\bar{\kappa}_s \bar{x}}, \quad \bar{A}_v \rightarrow e^{\bar{\kappa}_v \bar{x}}, \quad \bar{A}_0 \rightarrow e^{\bar{x}} \quad \text{as } \bar{x} \rightarrow -\infty, \quad (5.25)$$

where  $\bar{\Upsilon}_s = \Upsilon_s / |\Upsilon_s|$ ,  $\bar{\Upsilon}_v = \Upsilon_v / |\Upsilon_s|$ ,  $\bar{\Upsilon}_p = \Upsilon_p / |\Upsilon_p|$ , and

$$\chi \equiv \frac{\lambda_v}{\lambda_s} = |A_0^{(0)} \bar{\Upsilon}_s / \kappa_{0r}^4|^{\bar{\kappa}_{sr} - \bar{\kappa}_{vr}} \frac{|A_s^{(0)}|}{|A_v^{(0)}|}, \quad (5.26)$$

$$\phi = \arg A_0^{(0)} - \arg A_s^{(0)} - \arg A_v^{(0)} + (\bar{\kappa}_{si} + \bar{\kappa}_{vi}) \ln |A_0^{(0)} \bar{\Upsilon}_s / \kappa_{0r}^4|, \quad (5.27)$$

$$\tilde{\chi} = \bar{\kappa}_{0r}^{8\bar{\kappa}_{sr} - 7} |\bar{\Upsilon}_p| |\bar{\Upsilon}|^{-2\bar{\kappa}_{sr}} \frac{|A_s^{(0)}|^2}{|A_0^{(0)}|^{2\bar{\kappa}_{sr}}}.$$

Clearly,  $\chi$  represents the initial magnitude of the oblique varicose mode relative to that of the oblique sinuous mode,  $\phi$  the initial phase difference between the three waves, and  $\Delta$  the phase-velocity mismatching. The parameter  $\tilde{\chi}$  characterizes the initial amplitude of the oblique sinuous mode relative to the planar sinuous mode.

## 6. Application to a plane wake

Having presented the analysis for a general symmetric shear flow, we now specialize it to the flow with the profile (2.1). The advantage of choosing this profile is that it allows us to evaluate most of coefficients analytically. On the other hand, it fits the distribution of a typical wake reasonably well, as demonstrated by Mattingly & Criminale (1972). The two critical levels are located at the two inflexion points, say

$\pm y_c$ . For the profile (2.1),

$$y_c = \frac{1}{2} \ln(2 + \sqrt{3}), \quad \bar{U}'_c = \pm \frac{4}{3\sqrt{3}}, \quad \bar{U}'''_c = \mp \frac{16}{3\sqrt{3}}. \tag{6.1}$$

As shown in §1, the streamwise wavenumbers of the three participating modes in the triad are

$$\alpha_{s0} = 2, \quad \alpha_s = \frac{7}{4}, \quad \alpha_v = \frac{1}{4}.$$

For the neutral sinuous mode (2.2), it follows that  $y \rightarrow \pm y_c$ ,

$$\bar{\phi}_0 \rightarrow \frac{2}{3} \mp \frac{4}{3\sqrt{3}}(y \pm y_c) + \dots$$

A comparison with (3.10) indicates that the constants  $b_1$  and  $b_2$  can be identified as

$$b \equiv b_1 = b_2 = \frac{2}{3}. \tag{6.2}$$

A straightforward calculation gives

$$\tilde{J}_1 = \frac{4}{3}, \quad \tilde{J}_2 = 8[2 + \frac{1}{\sqrt{3}} \ln(2 + \sqrt{3})]. \tag{6.3}$$

Substituting (6.1)–(6.3) into (5.2) and (5.6), we obtain,

$$f_s = -8 \left[ \frac{\pi i}{\sqrt{3}} - 2 + \frac{1}{\sqrt{3}} \ln(2 + \sqrt{3}) \right],$$

$$\tilde{f} = \frac{8}{3} i \alpha_s c^{-1} + 8 \alpha_s^{-1} i \left[ \frac{\pi i}{\sqrt{3}} - 2 - \frac{1}{\sqrt{3}} \ln(2 + \sqrt{3}) \right],$$

$$f = \frac{8}{3} i \alpha_{s0} c^{-1} + 8 \alpha_{s0}^{-1} i \left[ \frac{\pi i}{\sqrt{3}} - 2 - \frac{1}{\sqrt{3}} \ln(2 + \sqrt{3}) \right].$$

Substitution of the above values together with (6.2) into (5.12) and (5.15) yields the coefficients  $\kappa_s$ ,  $Y_s$  and  $\kappa_0$ .

For the neutral varicose mode (2.3), it can be shown that as  $y \rightarrow \pm y_c$ ,

$$\phi_v \rightarrow \pm \frac{\sqrt{2}}{3} + \frac{\sqrt{6}}{9}(y \mp y_c) + \dots,$$

and hence it follows that

$$\hat{b} = \hat{b}_1 = -\hat{b}_2 = \frac{\sqrt{2}}{3}. \tag{6.4}$$

The integrals  $\hat{J}_1$  and  $\hat{J}_2$  are found to be

$$\hat{J}_1 = \frac{2}{3}, \quad \hat{J}_2 = -4 \left[ 1 - \frac{1}{\sqrt{3}} \ln(2 + \sqrt{3}) \right]. \tag{6.5}$$

It follows from (5.4) that

$$f_v = -4 \left[ \frac{\pi i}{\sqrt{3}} + 1 - \frac{1}{\sqrt{3}} \ln(2 + \sqrt{3}) \right],$$

$$\hat{f} = \frac{4}{3} i \alpha_v c^{-1} + 4 \alpha_v^{-1} i \left[ \frac{\pi i}{\sqrt{3}} + 1 - \frac{1}{\sqrt{3}} \ln(2 + \sqrt{3}) \right].$$

Substituting  $f_v$  and  $\hat{f}$  into (5.13), we obtain  $\kappa_v$  and  $Y_v$ .



The equation (3.41) subject to (3.40) and (3.42) is solved by a shooting method, which gives

$$\hat{D}_1 = \hat{D}_2 = \hat{D} \approx -0.452 .$$

The coefficient  $\Gamma_p$  is then calculated by using (5.14).

### 7. Study of the amplitude equations

#### 7.1. Very viscous limit: $\lambda \rightarrow \infty$

We consider the very viscous limit of the amplitude equations corresponding to  $\lambda \rightarrow \infty$ . This situation can occur when the initial magnitude of the planar sinuous mode is relatively small so that nonlinear effects come into play further downstream, i.e. closer to the neutral station than specified by (2.12). Consequently, the critical layers have already become equilibrium and viscous dominated when nonlinearity starts to assert its influence. By introducing the variable change  $\xi = \lambda^{-1/3}\tilde{\xi}$ ,  $\eta = \lambda^{-1/3}\tilde{\eta}$ , and taking the limit  $\lambda \rightarrow \infty$ , we find that the full equations (5.9), (5.10) and (5.11), to leading order, reduce to

$$\frac{d\check{A}_s}{d\check{x}} = \check{\kappa}_s\check{A}_s + \check{Y}_s\check{A}_0\check{A}_v^* , \tag{7.1}$$

$$\frac{d\check{A}_v}{d\check{x}} = \check{\kappa}_v\check{A}_v + \check{Y}_v\check{A}_0\check{A}_s^* + \check{Y}_p|\check{A}_s|^2\check{A}_v , \tag{7.2}$$

$$\frac{d\check{A}_0}{d\check{x}} = \check{\kappa}_0\check{A}_0 , \tag{7.3}$$

where

$$\check{x} = \lambda^{-1}x_1 , \tag{7.4}$$

$$\left. \begin{aligned} \check{\kappa}_s &= \lambda\kappa_s , & \check{\kappa}_v &= \lambda\kappa_v , & \check{\kappa}_0 &= \lambda\kappa_0 , \\ \check{A}_s &= \lambda^{-1/2}\tilde{A}_s , & \check{A}_v &= \lambda^{-1/2}\tilde{A}_v , & \check{A}_0 &= \tilde{A}_0 . \end{aligned} \right\} \tag{7.5}$$

Here the amplitude functions of the two oblique modes are rescaled so that the phase-locked feedback term is retained at leading order. The coefficients of the nonlinear terms are given by

$$\check{Y}_s = Y_s(\alpha_s^2\bar{U}_c^2\sigma_v)^{-1} , \quad \check{Y}_v = Y_v(\alpha_v^2\bar{U}_c^2\sigma_v)^{-1} , \quad \check{Y}_p = I_p Y_p ,$$

where

$$I_p = \left\{ \int_0^{+\infty} K_c(\xi) d\xi \right\} \left\{ \int_0^{+\infty} K_f(\eta) d\eta \right\} ,$$

with the parameter  $s$  in the kernels being assigned the value 1.

We now discuss the validity of the limiting amplitude equations (7.1)–(7.3). Equations (2.17) and (7.5) indicate that the growth rates of the three modes are  $O(\lambda^{-1}\epsilon^{1/4})$ . On the other hand, since  $\check{x} = O(1)$ ,  $x_1 = O(\lambda)$  (see (7.4)). It follows that the non-parallel-flow correction, i.e. the second term on the right-hand side of (2.21), is of  $O(\lambda^2\epsilon^{1/2})$ . Therefore, (7.1)–(7.3) remain valid as long as  $\lambda^2\epsilon^{1/2} \ll O(\lambda^{-1}\epsilon^{1/4})$ , i.e.

$$\lambda \ll O(R^{1/8}) , \tag{7.6}$$

as can be deduced after using (2.20). When  $\lambda \sim O(R^{1/8})$ , the non-parallel-flow correction will become a leading-order effect, i.e. it will be at the same order as the growth rate itself. Nevertheless, the appropriate amplitude equations for this latter

régime can be obtained by replacing the linear terms in (7.1)–(7.3) by  $(\gamma_s \bar{x} + A_s)$ ,  $(\gamma_v \bar{x} + A_v)$ , and  $(\gamma_0 \bar{x} + A_0)$  respectively, where  $\gamma_s$ ,  $A_s$ , etc. are some suitable constants. The nonlinear terms remain intact. Since this régime occurs at a much slower spatial scale, and hence may be of less importance, we shall not pursue it any further in the present paper.

7.2. Super-exponential growth induced by resonance

We now study the amplitude equations (5.22)–(5.24) with  $\tilde{\chi} = 0$ , which govern the parametric resonance stage and are valid when (2.19) holds. The solution to equation (5.24) simply is

$$\bar{A}_0 = e^{\bar{x}}. \tag{7.7}$$

Substituting  $\bar{A}_0$  into (5.22) and (5.23), we find that  $\bar{A}_s$  and  $\bar{A}_v$  have solutions of the form

$$\bar{A}_s = e^{\bar{\kappa}_s \bar{x}} \sum_{n=0}^{\infty} a_n^{(s)} e^{2n\bar{x}} + e^{\bar{\kappa}_v^* \bar{x}} \sum_{n=0}^{\infty} b_n^{(s)} e^{(2n+1)\bar{x}}, \tag{7.8}$$

$$\bar{A}_v = e^{\bar{\kappa}_v \bar{x}} \sum_{n=0}^{\infty} a_n^{(v)} e^{2n\bar{x}} + e^{\bar{\kappa}_s^* \bar{x}} \sum_{n=0}^{\infty} b_n^{(v)} e^{(2n+1)\bar{x}}, \tag{7.9}$$

where  $a_0^{(s)} = 1$  and  $a_0^{(v)} = 1$  so that the initial conditions (5.25) are satisfied. Substituting (7.8) and (7.9) into (5.22) and (5.23), and equating the coefficients of like powers, we obtain the recurrence relations

$$a_{n+1}^{(s)} = \frac{\chi e^{i\phi} \bar{Y}_s I_n(q)}{(2\sigma_v)^3 (n+1)(n+q)^3} b_n^{(v)}, \tag{7.10}$$

$$b_n^{(s)} = \frac{\chi e^{i\phi} \bar{Y}_s I_n^*(\bar{r})}{(\sigma_v)^3 (n+\bar{p}^*)(n+\bar{r}^*)^3} a_n^{(v)}, \tag{7.11}$$

$$a_{n+1}^{(v)} = \frac{\chi^{-1} e^{i\phi} \bar{Y}_v I_n(\bar{q})}{(2\sigma_v)^3 (n+1)(n+\bar{q})^3} b_n^{(s)}, \tag{7.12}$$

$$b_n^{(v)} = \frac{\chi^{-1} e^{i\phi} \bar{Y}_v I_n^*(r)}{(2\sigma_v)^3 (n+p^*)(n+r^*)^3} a_n^{(s)}, \tag{7.13}$$

where

$$p = (\bar{\kappa}_s - \bar{\kappa}_v^* + 1)/2, \quad q = \frac{\sigma_v + \bar{\kappa}_s \sigma_v + 1 - i\sigma_v \Delta}{2\sigma_v}, \quad r = \frac{\bar{\kappa}_s \sigma_v + \sigma - i\sigma_v \Delta}{2\sigma_v}, \tag{7.14}$$

$$\bar{p} = (\bar{\kappa}_v - \bar{\kappa}_s^* + 1)/2, \quad \bar{q} = \frac{\sigma_v + \bar{\kappa}_v \sigma_v + \sigma + i\sigma_v \Delta}{2\sigma_v}, \quad \bar{r} = \frac{\bar{\kappa}_v \sigma + 1 + i\sigma_v \Delta}{2\sigma_v}, \tag{7.15}$$

and  $I_n(q)$  is defined by

$$I_n(q) = 4\sigma_v^3 (n+q)^3 \int_0^{+\infty} \xi^2 e^{-s\sigma_v \xi^3 - 2\sigma_v (n+q)\xi} d\xi. \tag{7.16}$$

Note that  $I_n(q) \equiv 1$  when  $s = 0$  (the inviscid limit), and that for any  $s$ ,

$$I_n(q) \rightarrow 1 \quad \text{as} \quad n \rightarrow \infty. \tag{7.17}$$

It follows from (7.10) and (7.13) that

$$a_{n+1}^{(s)} = \frac{\bar{Y}_s \bar{Y}_v^* I_n(q) I_n(r)}{(2\sigma_v)^6 (n+1)(n+p)(n+q)^3 (n+r)^3} a_n^{(s)}, \tag{7.18}$$

where

$$\bar{\Gamma} = \bar{Y}_s \bar{Y}_v^* / (2\sigma_v)^6 .$$

Repeated use of (7.18) yields

$$a_n^{(s)} = \frac{\bar{\Gamma}^n}{n!(p)_n(q)_n^3(r)_n^3} \prod_{m=0}^{n-1} I_m(q)I_m(r) , \tag{7.19}$$

where we have defined  $(z)_n = \Gamma(z+n)/\Gamma(z)$  with  $\Gamma$  being the usual gamma function.

As in Goldstein & Lee (1992) and Wundrow *et al.* (1994), application of Laplace's method (Bender & Orszag 1980, p. 304) to the first sum in (7.8) with the coefficients (7.19) gives its asymptotic behaviour at large distance, namely

$$\sum_{n=0}^{\infty} a_n^{(s)} e^{2n\bar{x}} \rightarrow A_{\infty}^{(s)} \exp[-\frac{1}{4}(p+3q+3r-\frac{7}{2})\bar{x} + a_{\infty} e^{\bar{x}/4}] , \tag{7.20}$$

as  $\bar{x} \rightarrow +\infty$ , where

$$\left. \begin{aligned} A_{\infty}^{(s)} &= \frac{\Gamma(p)\Gamma^3(q)\Gamma^3(r)}{(2\pi)^{7/2}} (\frac{1}{8})^{1/2} (2\sigma_v)^{3(p+3q+3r-\frac{7}{2})/4} \prod_{m=0}^{\infty} I_m(q)I_m(r) , \\ a_{\infty} &= 8\bar{\Gamma}^{1/8} \end{aligned} \right\} \tag{7.21}$$

with  $|\arg \bar{\Gamma}^{1/8}| < \frac{1}{8}\pi$ . By a similar procedure, we can show that

$$\sum_{n=0}^{\infty} b_n^{(v)} e^{(2n+1)\bar{x}} \rightarrow \chi^{-1} e^{i(\phi+\arg \bar{Y}_v)} A_{\infty}^{*(s)} \exp[-\frac{1}{4}(p^*+3q^*+3r^*-\frac{7}{2})\bar{x} + a_{\infty}^* e^{\bar{x}/4}] , \tag{7.22}$$

$$\sum_{n=0}^{\infty} a_n^{(v)} e^{2n\bar{x}} \rightarrow A_{\infty}^{(v)} \exp[-\frac{1}{4}(\tilde{p}+3\tilde{q}+3\tilde{r}-\frac{7}{2})\bar{x} + a_{\infty}^* e^{\bar{x}/4}] , \tag{7.23}$$

$$\sum_{n=0}^{\infty} b_n^{(s)} e^{(2n+1)\bar{x}} \rightarrow \chi e^{i(\phi+\arg \bar{Y}_s)} A_{\infty}^{*(v)} \exp[-\frac{1}{4}(\tilde{p}^*+3\tilde{q}^*+3\tilde{r}^*-\frac{7}{2})\bar{x} + a_{\infty} e^{\bar{x}/4}] , \tag{7.24}$$

where

$$A_{\infty}^{(v)} = \frac{\Gamma(\tilde{p})\Gamma^3(\tilde{q})\Gamma^3(\tilde{r})}{(2\pi)^{7/2}} (\frac{1}{8})^{1/2} (2\sigma_v)^{3(\tilde{p}+3\tilde{q}+3\tilde{r}-7/2)/4} \prod_{m=0}^{\infty} I_m(\tilde{q})I_m(\tilde{r}) .$$

Substituting (7.20) and (7.22)–(7.24) into (7.8) and (7.9) and making use of (7.14) and (7.15), we finally obtain

$$\bar{A}_s \rightarrow \left( A_{\infty}^{(s)} + \chi e^{i(\phi+\arg \bar{Y}_s)} A_{\infty}^{*(v)} \right) \exp(b_{\infty}\bar{x} + a_{\infty} e^{\bar{x}/4}) , \tag{7.25}$$

$$\bar{A}_v \rightarrow \left( A_{\infty}^{(v)} + \chi^{-1} e^{i(\phi+\arg \bar{Y}_v)} A_{\infty}^{*(s)} \right) \exp(b_{\infty}^*\bar{x} + a_{\infty}^* e^{\bar{x}/4}) , \tag{7.26}$$

where

$$b_{\infty} = \frac{1}{8}(\kappa_s + \kappa_v^*) + \frac{3}{4}i . \tag{7.27}$$

Since the real part of  $a_{\infty}$  is always positive, (7.25) and (7.26) show that the resonance always causes the oblique sinuous and varicose modes to grow super-exponentially, regardless the values of the coefficients  $\bar{Y}_s$  and  $\bar{Y}_v$ . It is well known that super-exponential growth can occur through the usual parametric resonance of subharmonic

type (see e.g. Goldstein & Lee 1992; Wundrow *et al.* 1994). The analysis in this subsection can be regarded as an extension to the more general, non-subharmonic case.

As a result of the rapid amplification in the form of the super-exponential growth, the two oblique modes may eventually overtake the planar sinuous mode. Depending on the initial magnitude of the oblique modes, the subsequent stages can take two distinct forms. (a) If the magnitude of the oblique modes is algebraically small at the start of the parametric resonance, the oblique sinuous mode will soon grow to  $O(\epsilon^{7/8})$  to produce an extra back reaction on the oblique varicose mode through the phase-locked interaction. The evolution of the two oblique modes is then governed by the full equations (5.22) and (5.23), while the planar sinuous mode still evolves linearly. (b) If the oblique sinuous and varicose modes are exponentially small initially, then in the subsequent stage the planar sinuous mode can become nonlinear with its development governed by nonlinear critical-layer equations such as those of Goldstein & Hultgren (1989). On the other hand, the two oblique modes evolve over an inviscid spatial scale which is faster than that of the planar sinuous mode (cf. Wundrow *et al.* 1994). One can choose a distinguished magnitude for the oblique modes so that the phase-locked interaction between them also takes place in this stage.

Because the three-dimensional modes have smaller growth rates in the linear stage, scenario (b) is likely to occur in experiments. A complete understanding of this transition route requires more analytical and numerical work, and is a subject of our future study. The results obtained here for the parametric-resonance stage already indicate that the resonant triad of mixed modes may play an important rôle in causing transition in a plane wake. We wish to bring these results to the attention of the experimentalists with the hope that some experimental work could be devoted to it.

### 7.3. Numerical study of the amplitude equations

While the asymptotic analysis (for  $\tilde{\chi} = 0$ ) predicts the behaviour of the disturbance at large distance, it does not necessarily capture the transient feature of the development, nor is it valid for  $\tilde{\chi} \neq 0$ . For this reason, we integrate the (rescaled) amplitude equations (5.22) and (5.23) numerically using an Adams–Moulton (implicit) finite-difference scheme with sixth-order accuracy. As in Wu *et al.* (1993), the integrals over the infinite domains (see (5.22), (5.23)) are approximated by those over large but finite domains, the size of which is determined by trial and error.

The coefficients that we substitute in are those calculated for the profile (2.1). They depend on  $U_0$ , which in turn is related to the velocity deficit, an important parameter characterizing a plane wake. Both  $U_0$  and the velocity deficit vary considerably from the near field to the far wake. In our calculation, we choose  $U_0 = 3.667$ , which gives a deficit of 0.272, typical of the streamwise location where three-dimensional disturbances are observed to develop (e.g. Corke *et al.* 1992). For such a value of  $U_0$ , the linear growth rate of the oblique sinuous mode is about half that of the planar sinuous mode, while that of the oblique varicose mode is two magnitudes smaller (for  $\Delta = 0$ ). The other parameters are  $\chi$ ,  $\phi$ ,  $\lambda$ ,  $\Delta$  and  $\tilde{\chi}$ .

Since our primary interest is in the resonant-triad interaction, we first set  $\tilde{\chi} = 0$ . Our calculations show that depending on the size of  $\chi$ , which represents the magnitude of the oblique varicose mode relative to that of the oblique sinuous mode at the start of the resonance, two evolution scenarios can arise.

Given that the (oblique) varicose mode has a much smaller linear growth rate than the sinuous oblique mode, in natural transition  $\chi$  is likely to be small. So we first present the results for relatively small  $\chi$ . In figures 1 and 2, the parameter  $\Delta$  is set to zero, i.e. the phase velocities of the three modes are perfectly matched. Figure 1(a)

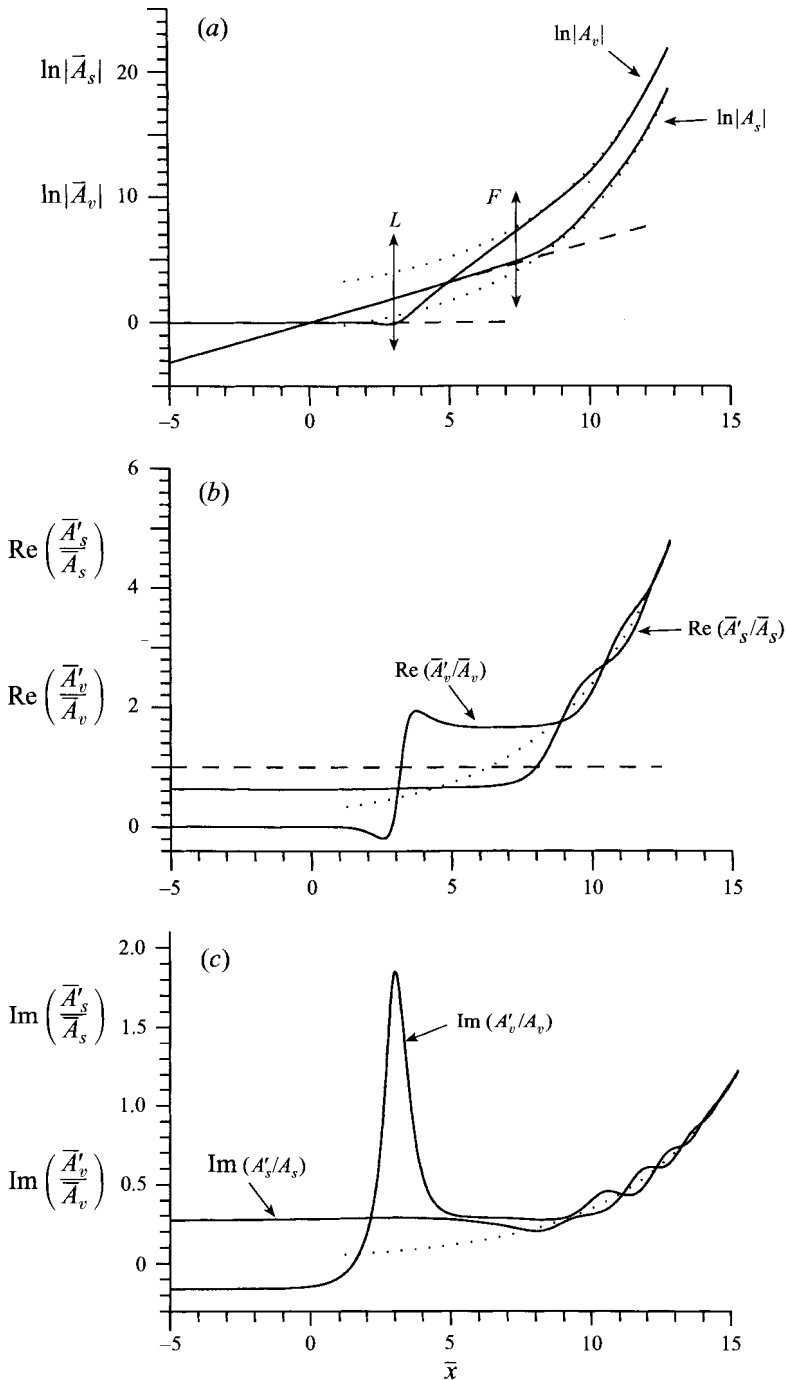


FIGURE 1. (a)  $\text{Ln}|\bar{A}_s|$  and  $\text{Ln}|\bar{A}_v|$  vs.  $\bar{x}$  for  $\Delta = 0$ ,  $\chi = 0.01$ ,  $\phi = 0$  and  $\lambda = 0$ . The dotted lines represent the large-distance asymptotic behaviours (7.25) and (7.26), and the dashed line the exponential growth. (b) The instantaneous growth rates  $\text{Re}(\bar{A}'_s/\bar{A}_s)$  and  $\text{Re}(\bar{A}'_v/\bar{A}_v)$  vs.  $\bar{x}$ . The dotted line represents the asymptotic result and the dashed line the scaled linear growth rate of the planar sinuous mode. (c) The wavenumber corrections  $\text{Im}(\bar{A}'_s/\bar{A}_s)$  and  $\text{Im}(\bar{A}'_v/\bar{A}_v)$  vs.  $\bar{x}$ . The dotted line represents the asymptotic result.

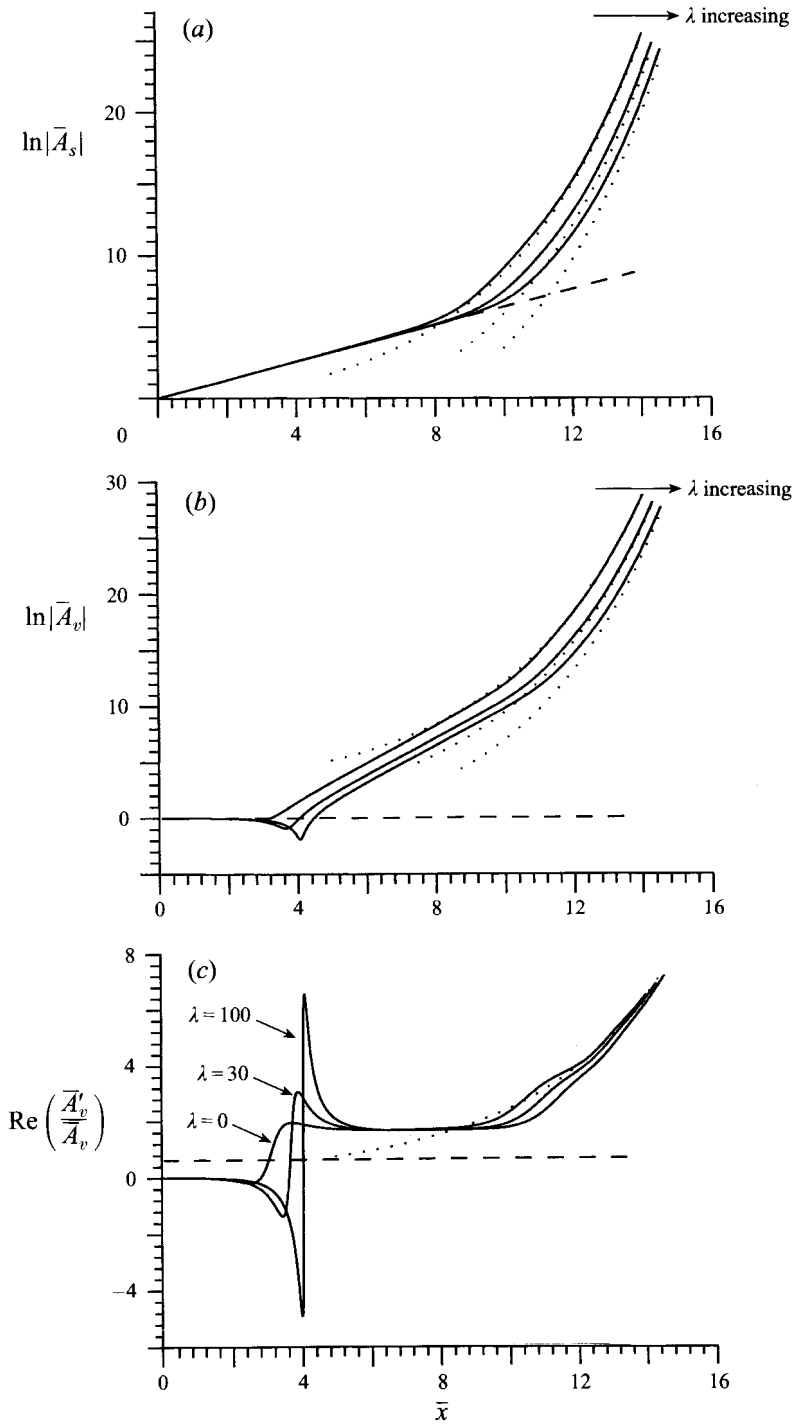


FIGURE 2(a-c). For caption see facing page.

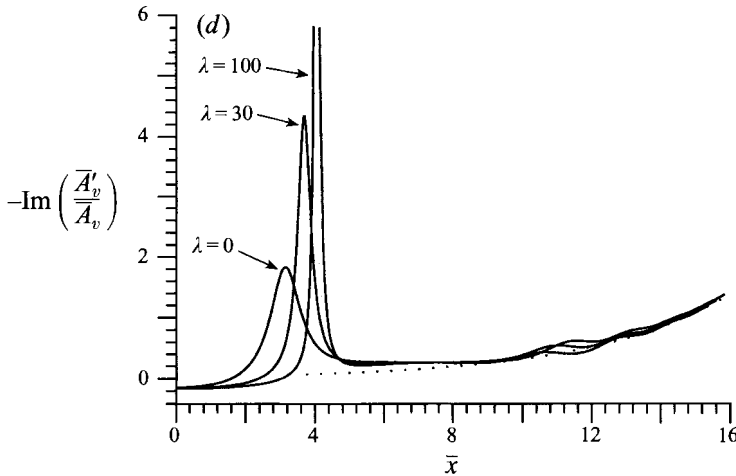


FIGURE 2. (a)  $\text{Ln}|\bar{A}_s|$  vs.  $\bar{x}$  for  $\Delta = 0$ ,  $\lambda = 0$ ,  $\lambda = 30$  and  $\lambda = 100$ . The dotted lines represent the asymptote (7.25), and the dashed line the exponential growth. (b)  $\text{Ln}|\bar{A}_v|$  vs.  $\bar{x}$  for  $\lambda = 0$ ,  $\lambda = 30$  and  $\lambda = 100$ . The dotted lines represent the asymptote (7.26), and the dashed line the exponential growth. (c) The instantaneous growth rate  $\text{Re}(\bar{A}'_v/\bar{A}_v)$  vs.  $\bar{x}$ . The dotted line represents the asymptotic result and the dashed line the scaled linear growth rate of the oblique sinuous mode. (d) The wavenumber correction  $\text{Im}(\bar{A}'_v/\bar{A}_v)$  vs.  $\bar{x}$ . The dotted line represents the asymptotic result. A 'gap' appears because we cut off the high peak in order to accommodate the picture with an appropriate graphical resolution.

shows the downstream development of  $\bar{A}_s$  and  $\bar{A}_v$  for  $\chi = 0.01$  and  $\lambda = 0$  (inviscid limit). The result is representative for  $\chi \leq 0.1$ . As illustrated, the disturbance evolves through *three* distinct stages. The first is the linear stage, in which all modes evolve independently. The gain in the amplitude of the oblique varicose mode is hardly appreciable because its linear growth rate is very small. On reaching  $L$ , the disturbance enters the second stage in which the two sinuous modes have attained a certain magnitude so that they interact to enhance the growth of the varicose mode. An interesting feature is that the varicose mode evolves almost exponentially over a considerable distance, but with a rate two magnitudes larger than its linear growth rate, and twice that of the oblique sinuous mode. At the same time, the sinuous oblique mode still follows linear theory up to point  $F$ . This is because before reaching  $F$ , the varicose mode is too weak to produce any significant feedback effect on the oblique sinuous mode. The third stage starts from  $F$ , in which both sinuous and varicose oblique modes become sufficiently large so that they are coupled through the interaction with the plane sinuous mode, and undergo rapid amplification simultaneously. Finally, they both approach the super-exponential growth, confirming the prediction of the large-distance asymptotic analysis. The development of each mode is revealed more clearly by their instantaneous growth rates  $\text{Re}(\bar{A}'/\bar{A})$  in figure 1(b). It shows that following the linear stage, the growth rate of the varicose mode changes abruptly, and then remains almost constant for a rather long distance, corresponding to the 'quasi-exponential' growth of  $\bar{A}_v$  noted earlier. Note also that the sudden change of the growth rate is accompanied by abrupt adjustment of the wavenumber correction  $\text{Im}(\bar{A}'_v/\bar{A}_v)$ , as shown in figure 1(c).

We have also performed calculations for other values of  $\phi$ , and find that the qualitative features of the development persist, although for some  $\phi$  the growth rate and wavenumber correction of the oblique varicose mode adjust themselves in a more violent manner than those shown in figure 1(b,c).

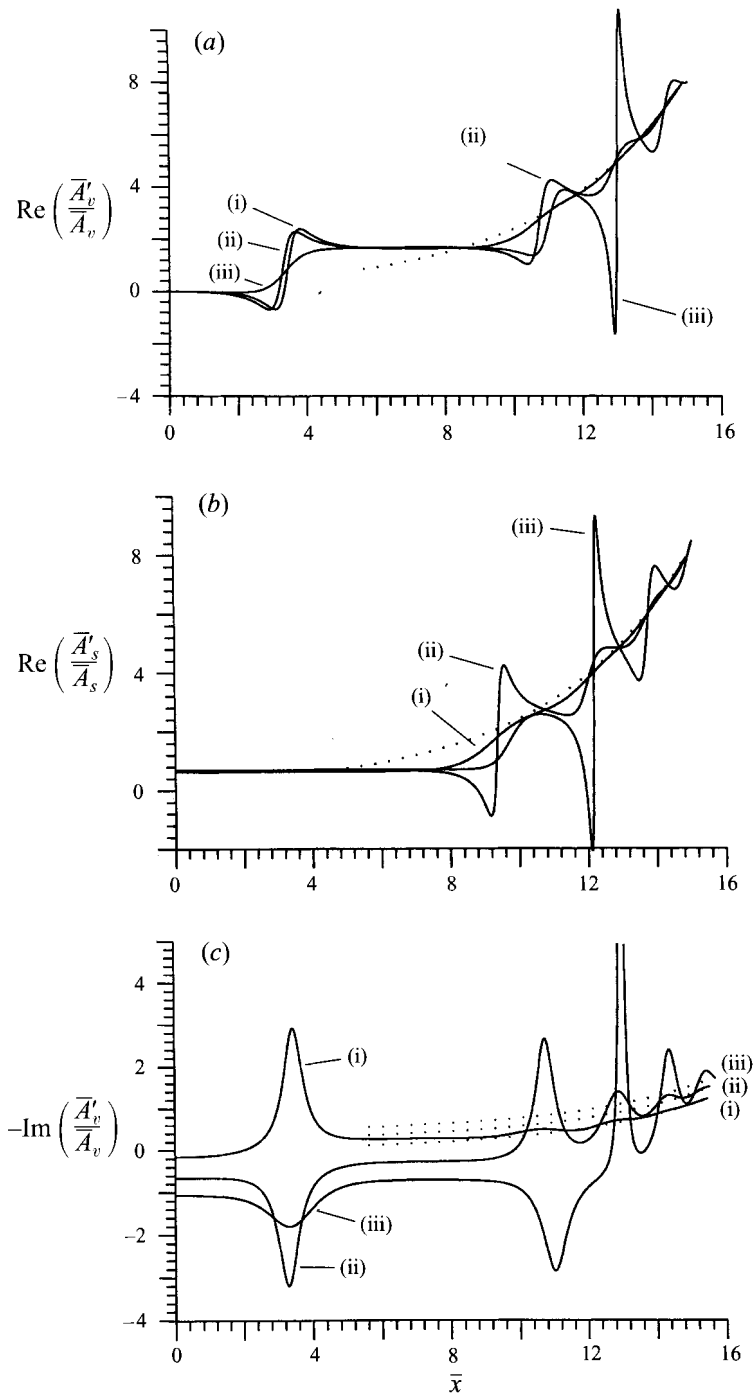


FIGURE 3(a-c). For caption see facing page.



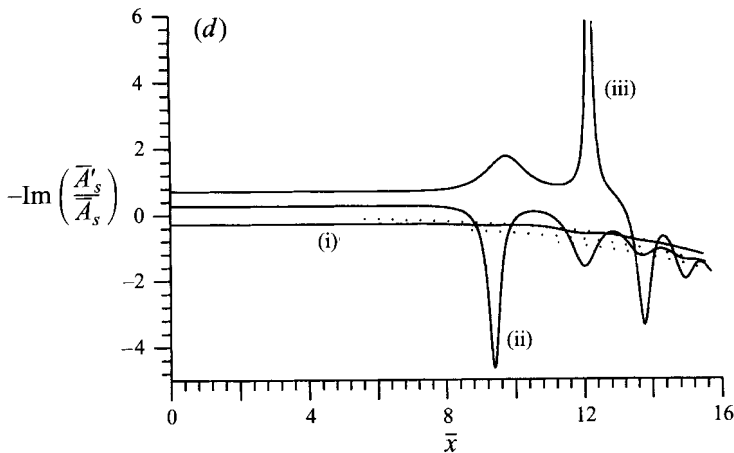


FIGURE 3. Effect of phase-speed mismatching: (a)  $\text{Re}(\bar{A}'_v/\bar{A}'_v)$  vs.  $\bar{x}$ ; (b)  $\text{Re}(\bar{A}'_s/\bar{A}'_s)$  vs.  $\bar{x}$ ; (c)  $-\text{Im}(\bar{A}'_v/\bar{A}'_v)$  vs.  $\bar{x}$ ; (d)  $-\text{Im}(\bar{A}'_s/\bar{A}'_s)$  vs.  $\bar{x}$ . Curves (i), (ii) and (iii) correspond to  $\Delta = 0, 0.5$  and  $0.9$  respectively, while the dotted lines represent the asymptotic behaviours. Other parameters are  $\chi = 0.01$ ,  $\phi = 0$  and  $\lambda = 10$ . A gap appears in (c) for the same reason as in figure 2(d).

The effect of viscosity parameter  $\lambda$  is investigated. Figures 2(a) and 2(b) show the development of the oblique sinuous and varicose modes respectively for three different values of  $\lambda$ . As expected, viscosity acts to delay the position at which the resonance starts to take place, but cannot suppress the ultimate super-exponential growth. In figures 2(c) and 2(d), we plot  $\text{Re}(\bar{A}'_v/\bar{A}'_v)$  and  $\text{Im}(\bar{A}'_v/\bar{A}'_v)$  respectively. It is interesting to note that as viscosity increases, the growth rate and the wavenumber correction become more and more spiky during the adjustment. This is in contrast to the intuitive expectation that viscosity has a smoothing effect. Another feature worth noting is that for different values of  $\lambda$ , the curves of  $\text{Re}(\bar{A}'_v/\bar{A}'_v)$  are pinched together, indicating that the 'quasi-exponential' growth rate is largely independent of viscosity, or of Reynolds number.

The effect of mismatching of phase speeds  $\Delta$  is shown in figure 3(a-d). It is seen that phase-speed mismatching can cause the instantaneous growth rates (figure 3a,b) and the wavenumber corrections (figure 3c,d) of the oblique varicose and sinuous modes to oscillate before they approach the super-exponential growth stage. Phase-speed mismatching also smooths the 'jump' of the growth rate of the oblique varicose mode (see figure 3a). Nevertheless, the 'quasi-exponential' growth of the oblique varicose mode persists for different values of  $\Delta$ , and is hardly affected by this effect.

We now turn to the case where  $\chi$  is relatively large. This situation may occur when the varicose oblique mode is preferentially excited. (It is possible to excite sinuous and various modes independently (Marasli *et al.* 1989).) The amplitude evolution and the instantaneous growth rates are displayed in figures 4(a) and 4(b) respectively for  $\chi = 2.0$  in the inviscid limit ( $\lambda = 0$ ). A comparison with figures 1(a) and 1(b) indicates that the evolution scenario is different from the small- $\chi$  case in the sense that the disturbance now evolves through *four* stages. The first is of course linear. However, following the linear stage, i.e. between points *L* and *P*, it is the sinuous oblique mode rather than the varicose oblique mode that experiences an enhanced growth. The difference arises because the varicose mode now has a relatively large initial magnitude so that it first interacts with the planar sinuous mode to accelerate the oblique sinuous

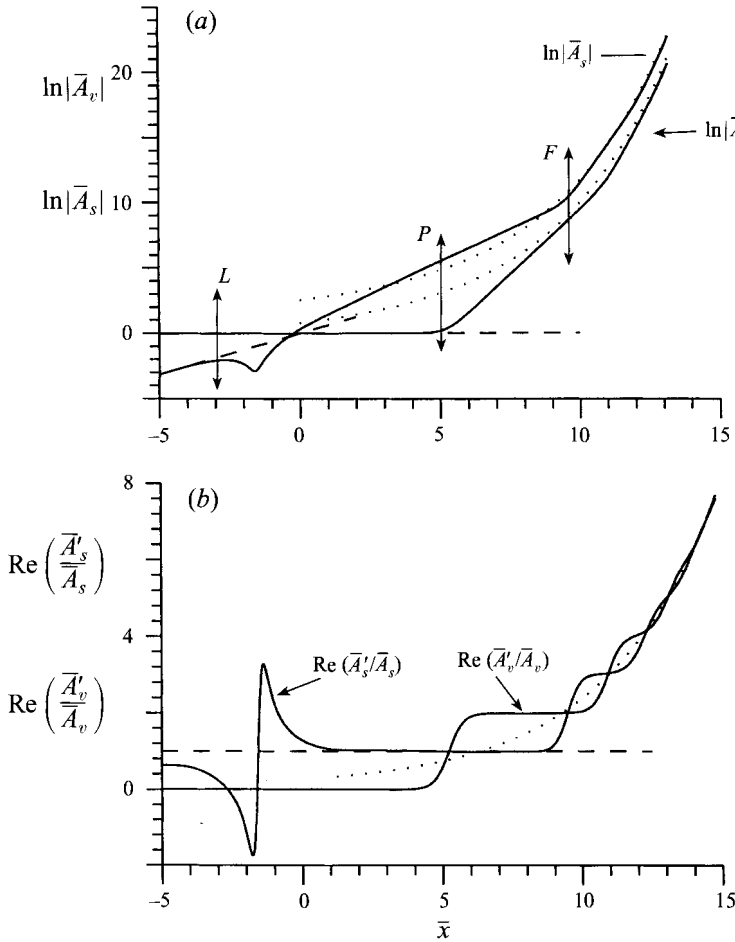
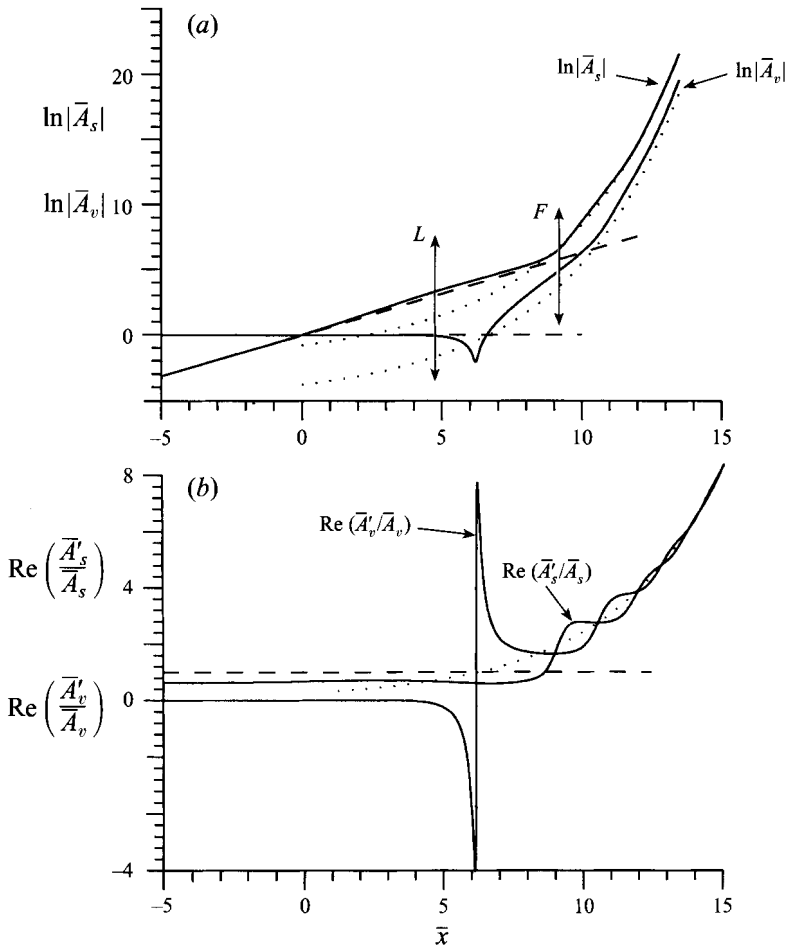


FIGURE 4. (a)  $\text{Ln}|\bar{A}_s|$  and  $\text{Ln}|\bar{A}_v|$  vs.  $\bar{x}$  for  $\Delta = 0$ ,  $\chi = 2.0$ ,  $\phi = 30^\circ$  and  $\lambda = 0$ . The dotted lines represent the large-distance asymptotic behaviours (7.25) and (7.26), and the dashed line the exponential growth. (b) The instantaneous growth rates  $\text{Re}(\bar{A}'_s/\bar{A}_s)$  and  $\text{Re}(\bar{A}'_v/\bar{A}_v)$  vs.  $\bar{x}$ . The dotted line represents the asymptotic result and the dashed line the scaled linear growth rate of the planar sinuous mode.

mode. Figure 4(b) indicates that the oblique sinuous mode evolves exponentially in the second stage, with a rate almost identical to that of the planar sinuous mode. Once the sinuous oblique mode has grown to a certain extent, it then causes the varicose mode to amplify rapidly, again in a quasi-exponential manner with a rate twice that of the sinuous oblique mode. This third stage (between  $P$  and  $F$  in figure 4a) and the fourth stage (starting from  $F$ ) are similar to the second and third stages in the small- $\chi$  case respectively. The extra stage in the present case, i.e. stage two, serves to compensate the small initial magnitude of the oblique sinuous mode. Calculations with viscosity included reveal that the above scenario is fragile in the sense that a small viscosity can eliminate the second stage. For example, when  $\lambda = 2$ , the oblique sinuous mode no longer undergoes an enhanced growth prior to the varicose mode, as shown in figure 5(a,b). On the contrary, the first effect of the resonance is to promote the varicose mode.

Finally, we investigate the rôle of the phase-locked feedback term by examining the development of the oblique modes at different values of  $\tilde{\chi}$ . As figure 6(a,b)

FIGURE 5. As figure 4 but for  $\lambda = 2$ .

illustrates, for small and moderate  $\tilde{\chi}$ , the enhanced growth in the earlier stages is largely induced by the resonant-triad interaction, while the phase-locked interaction is negligible. However, once the oblique modes become sufficiently large, the phase-locked interaction comes into play, causing the oblique varicose mode to evolve more rapidly than the super-exponential growth (see figure 6a). Although the phase-locked interaction contributes a term only to the amplitude equation of the oblique varicose mode, its effect is also felt by the oblique sinuous mode through the resonance term. As a result, the development of the latter mode is further enhanced (figure 6b).

## 8. Conclusion and discussion

In this paper, we have shown that by choosing appropriate sinuous and varicose modes of a symmetric shear flow, they can form an active resonant triad of non-subharmonic form. The development of the triad is studied in the non-equilibrium critical-layer régime. We show that the resonance can induce interesting and intriguing transient growth, and may eventually lead to super-exponential growth in the amplitudes of the oblique sinuous and varicose modes. The possible subsequent stages are

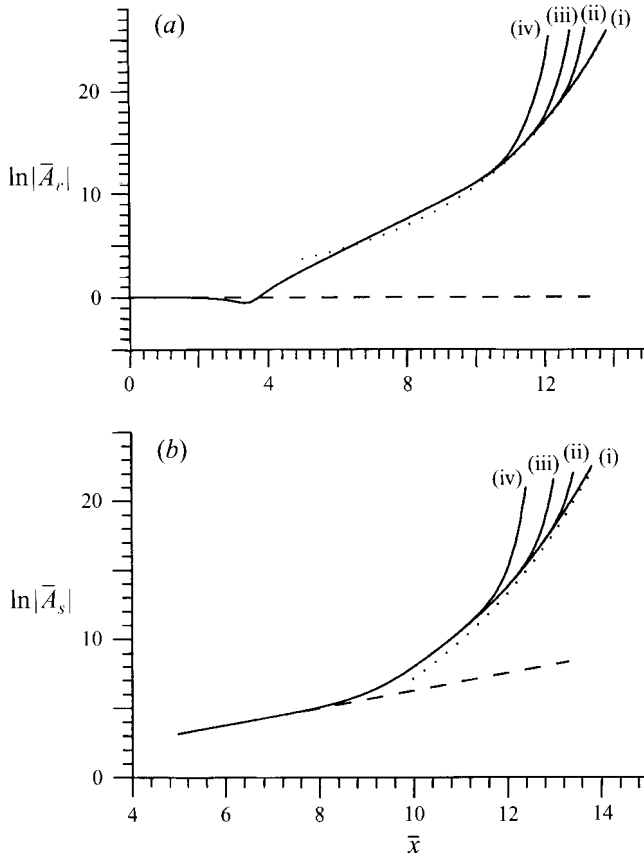


FIGURE 6.  $\text{Ln}|\tilde{A}_v|$  and  $\text{Ln}|\tilde{A}_s|$  vs.  $\bar{x}$  for different values of  $\tilde{\chi}$ : (i)  $\tilde{\chi} = 0$ , (ii)  $\tilde{\chi} = 10^{-4}$ , (iii)  $\tilde{\chi} = 10^{-2}$ , (iv)  $\tilde{\chi} = 1$ . The other parameters are  $\Delta = \phi = 0$ ,  $\chi = 0.01$ ,  $\lambda = 10$ . The dotted lines represent the asymptotes (7.25) and (7.26) respectively, and the dashed lines the exponential growth.

pointed out with their features being highlighted. We suggest that such a resonance may provide a possible explanation for the development of three-dimensional varicose modes. This resonance, together with the phase-locked interaction (Wu & Stewart 1996a) and the side-band instability (Wu & Stewart 1996b) may represent three major mechanisms which cause rapid amplification of three-dimensional disturbances in a plane wake.

Our results show that although in the linear régime the varicose mode has a smaller growth rate, its development can be significantly enhanced by the sinuous modes through nonlinear resonance. Consequently, sufficiently far downstream it attains the same evolution behaviour as the oblique sinuous mode as indicated by (7.25) and (7.26). Moreover, it follows from (5.18), (5.19), (5.26), (7.25) and (7.26) that as  $\bar{x} \rightarrow +\infty$ ,

$$|\tilde{A}_v/\tilde{A}_s| \rightarrow \left| \chi A_\infty^{(v)} + e^{i(\phi + \arg \tilde{\gamma}_v)} A_\infty^{*(s)} \right| / \left| A_\infty^{(s)} + \chi e^{i(\phi + \arg \tilde{\gamma}_s)} A_\infty^{*(v)} \right|.$$

The right-hand side is of order one except for some special values of  $\chi$  and  $\phi$ . This implies that in general the ratio of the (unscaled) magnitude of the varicose mode to that of the sinuous oblique mode approaches an  $O(1)$  constant. This is so even when

$\chi \rightarrow 0$ . Therefore, no matter how small the varicose mode initially is, it cannot be dismissed if the transition processes far downstream are to be understood.

For the wake with the profile (2.1), the frequency of the oblique sinuous mode differs from that of the planar sinuous mode only by 12.5%, and hence can be regarded as within the side-band of the latter mode, while the oblique varicose mode is the  $\frac{1}{8}$ -subharmonic. Therefore, according to our results, two peaks are expected to appear in the energy spectrum of the disturbance with one centred at the frequency of the most unstable sinuous mode, while the other is at the  $\frac{1}{8}$ -subharmonic. We note that two such peaks are eminent in figure 8 of Sato & Saito (1978). Unfortunately, a detailed quantitative comparison is not yet possible because of the lack of relevant experimental data. Clearly, more experimental work is needed in order to confirm the rôle of the resonance identified in this paper.

Given that the usual subharmonic resonance (of sinuous modes) is inactive, there is no reason to expect the  $\frac{1}{2}$ -subharmonic to play a special rôle. Indeed, Sato (1970) and Sato & Saito (1978) pointed out that the disturbance in a flat-plate wake does not contain a predominant  $\frac{1}{2}$ -subharmonic. However, secondary instability theory (Herbert 1988 and references therein) tends to suggest that a  $\frac{1}{2}$ -subharmonic should develop. Based on such a consideration, Corke *et al.* (1992) excited a pair of oblique subharmonics as well as a planar fundamental wave and mapped out the downstream evolution of each mode. They observed that the subharmonics exhibited an enhanced amplification and attributed this to the secondary instability mechanism based on Floquet theory. However, although the measured growth rate of the subharmonics is much larger than that predicted by linear theory, it is comparable to that of the planar fundamental. Therefore, there is little justification for treating the fundamental as being quasi-steady. Recently, Wu & Stewart (1996a) suggest that the experimental results of Corke *et al.* (1992) can be explained by phase-locked interaction, in which the evolving nature of the fundamental is taken into account properly. In this theory, the  $\frac{1}{2}$ -subharmonic does not have a special status in the sense that other oblique modes, provided that they are phase-locked with the planar mode, can be amplified in the same manner.

The rôle of three-dimensional subharmonics was also investigated by Lasheras & Meiburg (1990) by using an inviscid vortex method. While it is found that the interaction between the fundamental and the subharmonic can lead to distinct vortex structures, there is no direct evidence to suggest that the energy growth of the subharmonic is accelerated by the fundamental through resonance. The temporal development of the two-dimensional subharmonic† was simulated by Chen *et al.* (1990) for a compressible wake of low Mach number. Their results show that the subharmonic overtakes the fundamental when the latter starts to decay. However, the growth rate of the former never exceeds the value given by linear theory. This perhaps indicates that the two-dimensional subharmonic resonance (i.e. the Kelly type of resonance) is insignificant in a plane wake, a conclusion consistent with the result of Leib & Goldstein (1989).

† The two-dimensional subharmonic is also studied by Meiburg (1987) via a discrete vortex model. However his results are related to the vortex pairing process in the near wake of a bluff body, rather than to transition, which occurs further downstream where the von Karman vortices have almost completely died away; see e.g. Cimbala *et al.* (1988). Nevertheless, it is interesting to note that in Meiburg's model, the subharmonic introduced into the upper layer is not in phase with that in the lower layer so that the symmetry about the centreline of the wake is broken. In some sense, this can be interpreted as the subharmonic consisting of both the sinuous and varicose components.

Finally, we point out that the idea of including sinuous and varicose modes so that they form an active resonant triad can be applied to compressible symmetric shear flows. The calculations of Chen *et al.* (1990) show that for a compressible wake, two-dimensional modes still have larger linear growth rates. Therefore, an explanation of the development of three-dimensional disturbances relies on nonlinear mechanisms, for which the resonant triad of mixed modes is a possible candidate. However, because of the compressibility effect, the Squire transformation is no longer applicable. A detailed study of the dispersion relations of both the sinuous and varicose modes is necessary in order to establish the existence of such a triad. We plan to investigate this aspect in the future.

The author would like to thank Mr P. A. Stewart for his suggestion of using the scaling (2.18) to include the phase-locked interaction effect. Thanks are also due to Professors J. T. Stuart, D. W. Moore, Dr S. J. Cowley for helpful discussions, to Dr M. E. Goldstein for his encouragement, and to referees for comments. This research is supported by a Nuffield Foundation award for newly appointed science lecturers.

## Appendix.

The quadratic interaction between the oblique sinuous and varicose modes generates, through the jump (A 5), an  $O(\delta^2\mu^{-3})$  difference mode in the main part of the flow. The  $O(\delta^2\mu^{-3})$  pressure in turn drives  $O(\delta^2\mu^{-4})$  streamwise and spanwise velocities in the critical layers, i.e.  $\hat{U}_f$  and  $\hat{W}_f$  in (4.1) and (4.3). It is found that

$$\hat{U}_f = -\bar{U}'_c \sin^2\theta_f \Pi_f^{(0)}, \quad \hat{W}_f = i\bar{U}'_c \sin\theta_f \cos\theta_f \Pi_f^{(0)}, \quad (\text{A } 1)$$

where

$$\Pi_f^{(n)} = \int_0^{+\infty} \xi^n D_f(x_1 - \xi, T - \xi) e^{-s_f \xi^3 - i\Omega_f \xi} d\xi, \quad (\text{A } 2)$$

$$\Omega_f = \alpha_f \bar{U}'_c Y, \quad s_f = \frac{1}{3} \lambda \alpha_f^2 \bar{U}'_c{}^2. \quad (\text{A } 3)$$

The  $O(\delta^2\mu^{-2})$  term in (4.2),  $V_1$ , and  $O(\delta^2\mu^{-3})$  terms in (4.1) and (4.3),  $W_1$  and  $W_1$ , are velocities directly driven by the Reynolds stresses produced by the interaction between the two oblique modes. As far as deriving the amplitude equation is concerned, we only need to solve for  $V_1$ . It takes the form

$$V_1 = \hat{V}_1 e^{i(\alpha_f \zeta - 2\beta z)} + \tilde{V}_1 e^{i\alpha_0 \zeta},$$

where the second term on the right-hand side is associated with the sum mode, which, unlike the difference mode, is two-dimensional and does not play an active role (cf. Wu & Stewart 1996a). The function  $\hat{V}_1$  satisfies

$$\hat{L}_{\alpha_f} \hat{V}_{1,Y Y} = i\alpha_{s0} \alpha_v^2 \bar{U}'_c{}^3 \sin^2\theta_v [A_s \Pi_v^{*(2)} - 2i\alpha_{s0} (\alpha_v^2 \bar{U}'_c)^{-1} \sin^2\theta (\Pi_s^{(0)} \Pi_v^{*(0)})_Y]. \quad (\text{A } 4)$$

Solving the above equation and matching it to the outer solution, we find that

$$C_j^+ - C_j^- = A_f(x_1, T), \quad (\text{A } 5)$$

where

$$A_f = h_f \int_0^{+\infty} K_f(\xi) A_s(x_1 - \xi, T - \xi) A_v^*(x_1 - \sigma\xi, T - \sigma\xi) d\xi, \quad (\text{A } 6)$$

$$h_f = 2\pi i \alpha_{s0} \alpha_f^2 \alpha_v^{-1} \bar{U}'_c |\bar{U}'_c| \sin^2\theta_v b_j \hat{b}_j^* ;$$

the kernel function  $K_f$  is defined by

$$K_f(\xi) = \xi^2 e^{-s_f \sigma \xi^3} - 2\alpha_{s0} \alpha_f^{-1} \sin^2 \theta \int_0^\xi (\zeta - \xi) e^{-s \zeta^3 - s_v(\zeta + \sigma_f \zeta)^3 - s_f(\zeta - \xi)^3} d\zeta, \quad (\text{A } 7)$$

and

$$\sigma_s = \alpha_{s0}/\alpha_s, \quad \sigma_v = \alpha_{s0}/\alpha_v, \quad \sigma = \alpha_s/\alpha_v, \quad \sigma_f = \alpha_f/\alpha_v. \quad (\text{A } 8)$$

#### REFERENCES

- BENDER, C. M. & ORSZAG, S. A. 1978 *Advanced Mathematical Methods for Scientists and Engineers*. McGraw-Hill.
- CHEN, J. H., CANTWELL, B. J. & MANSOUR, N. N. 1990 The effect of Mach number on the stability of a plane supersonic wake. *Phys. Fluids A* **2**, 984–1004.
- CIMBALA, J. M., NAGIB, H. M. & ROSHKO, A. 1988 Large structure in the far wake of two-dimensional bluff bodies. *J. Fluid Mech.* **190**, 265–298.
- CORKE, T. C., KRULL, J. D. & GHASSEMI, M. 1992 Three-dimensional-mode resonance in far wakes. *J. Fluid Mech.* **239**, 99–132.
- COWLEY, S. J. & WU, X. 1994 Asymptotic approaches to transition modelling. In *Progress in Transition Modelling*, AGARD Rep. 793.
- CRAIK, A. D. D. 1971 Non-linear resonant instability in boundary layers. *J. Fluid Mech.* **50**, 393–413.
- DRAZIN, P. G. & HOWARD, L. N. 1966 Hydrodynamic stability of parallel flow of inviscid flow. *Adv. Appl. Mech.* **9**, 1–89.
- GOLDSTEIN, M. E. 1994 Nonlinear interaction between oblique waves on nearly planar shear flows. *Phys. Fluids A* **6**, 42–65.
- GOLDSTEIN, M. E. & CHOI, S.-W. 1989 Nonlinear evolution of interacting oblique waves on two-dimensional shear layers. *J. Fluid Mech.* **207**, 97–120. Corrigendum, *J. Fluid Mech.* **216**, 1990, 659–663.
- GOLDSTEIN, M. E. & HULTGREN, L. S. 1989 Nonlinear spatial evolution of an externally excited instability wave in a free shear layer. *J. Fluid Mech.* **197**, 295–330.
- GOLDSTEIN, M. E. & LEE, S. S. 1992 Fully coupled resonant-triad interaction in an adverse-pressure-gradient boundary layer. *J. Fluid Mech.* **245**, 523–551.
- GOLDSTEIN, M. E. & LEE, S. S. 1993 Oblique instability waves in nearly parallel shear flows. In *Nonlinear Waves and Weak Turbulence with Applications in Oceanography and Condensed Matter Physics* (ed. N. Fitzmaurice, D. Gurarie, F. McCaughan & W. Woyczynski), pp. 159–177. Birkhauser.
- GOLDSTEIN, M. E. & LEIB, S. J. 1989 Nonlinear evolution of oblique waves on compressible shear layers. *J. Fluid Mech.* **207**, 73–96.
- HABERMAN, R. 1972 Critical layers in parallel shear flows. *Stud. Appl. Maths* **50**, 139.
- HERBERT, T. 1988 Secondary instability of boundary layers. *Ann. Rev. Fluid Mech.* **20**, 487–526.
- KELLY, R. E. 1968 On the resonant interaction of neutral disturbances in two inviscid shear flows. *J. Fluid Mech.* **31**, 789–799.
- KO, D., KUBOTA, T. & LEES, L. 1970 Finite disturbance effect on the stability of a laminar incompressible wake behind a flat plate. *J. Fluid Mech.* **40**, 315–341.
- LASHERAS, J. C. & MEIBURG, E. 1990 Three-dimensional vorticity modes in the wake of a flat plate. *Phys. Fluids A* **2**, 371–380.
- LEE, S. S. 1994 Critical-layer analysis of fully coupled resonant-triad interaction in a boundary layer. *Submitted to J. Fluid Mech.*
- LEIB, S. J. & GOLDSTEIN, M. E. 1989 Nonlinear interaction between the sinuous and varicose instability modes in a plane wake. *Phys. Fluids A* **1**, 513–521.
- MALLIER, R. 1995 Fully coupled resonant triad interactions in a Bickley jet. *Submitted to Eur. J. Mech.*
- MALLIER, R. & MASLOWE, S. A. 1994 Fully coupled resonant triad interactions in a free shear layer. *J. Fluid Mech.* **278**, 101–121.
- MANKBADI, R. R., WU, X. & LEE, S. S. 1993 A critical-layer analysis of the resonant triad in Blasius boundary-layer transition: nonlinear interactions. *J. Fluid Mech.* **256**, 85–106.

- MARASLI, B., CHAMPAGNE, F. H. & WYGNANSKI, I. J. 1989 Modal decomposition of velocity signals in a plane, turbulent wake. *J. Fluid Mech.* **198**, 255–273.
- MATTINGLY, G. E. & CRIMINALE, W. O. 1972 The stability of an incompressible two-dimensional wake. *J. Fluid Mech.* **51**, 233–272.
- MEIBURG, E. 1987 On the role of subharmonic perturbations in the far wake. *J. Fluid Mech.* **177**, 83–107.
- MIKSAD, R. W., JONES, F. L., POWERS, E. J., KIM, Y. C. & KHADRA, L. 1982 Experiments on the role of amplitude and phase modulation during transition to turbulence. *J. Fluid Mech.* **123**, 1–29.
- RAETZ, G. S. 1959 A new theory of the cause of transition in fluid flows. Northrop Corp. NOR-59-383 BLC-121.
- SATO, H. 1970 An experimental study of nonlinear interaction of velocity fluctuations in the transition region of a two-dimensional wake. *J. Fluid Mech.* **44**, 741–765.
- SATO, H. & KURIKI, K. 1961 The mechanism of transition in the wake of a thin flat plate placed parallel to a uniform flow. *J. Fluid Mech.* **11**, 321–353.
- SATO, H. & SAITO, H. 1975 Fine-structure of energy spectra of velocity fluctuations in the transition region of a two-dimensional wake. *J. Fluid Mech.* **67**, 539–559.
- SATO, H. & SAITO, H. 1978 Artificial control of the laminar-turbulent transition of a two-dimensional wake by external sound. *J. Fluid Mech.* **84**, 657–572.
- WILLIAMSON, C. H. K. & PRASAD, A. 1993a A new mechanism for oblique wave resonance in the 'natural' far wake. *J. Fluid Mech.* **256**, 269–313.
- WILLIAMSON, C. H. K. & PRASAD, A. 1993b Acoustic forcing of oblique wave resonance in the far wake. *J. Fluid Mech.* **256**, 315–341.
- WU, X. 1992 The nonlinear evolution of high-frequency resonant-triad waves in an oscillatory Stokes-layer at high Reynolds number. *J. Fluid Mech.* **245**, 553–597.
- WU, X. 1993 On critical-layer and diffusion-layer nonlinearity in the three-dimensional stage of boundary-layer transition. *Proc. R. Soc. Lond. A* **433**, 95–106.
- WU, X. 1995 Viscous effects on fully-coupled resonant triad interactions: an analytical approach. *J. Fluid Mech.* **292**, 377–407.
- WU, X., LEE, S. S. & COWLEY, S. J. 1993 On the weakly nonlinear three-dimensional instability of shear flows to pairs of oblique waves: the Stokes layer as a paradigm. *J. Fluid Mech.* **253**, 681–721.
- WU, X. & STEWART, P. A. 1996a Interaction of phase-locked modes: a new mechanism for the rapid growth of three-dimensional disturbances. *J. Fluid Mech.* **316**, 335–372.
- WU, X. & STEWART, P. A. 1996b Side-band instability of growing waves. *To be submitted to Phys. Fluids*.
- WUNDROW, D. W., HULTGREN, L. S. & GOLDSTEIN, M. E. 1994 Interaction of oblique stability waves with a nonlinear planar wave. *J. Fluid Mech.* **264**, 343–372.
- WYGNANSKI, I., CHAMPAGNE, F. & MARASLI, B. 1986 On the large-scale structures in two-dimensional small-deficit, turbulent wakes. *J. Fluid Mech.* **168**, 31–71.